UC San Diego

UC San Diego Electronic Theses and Dissertations

Title

Exploring Drug-Inducible BDNF in Promoting Regeneration and Guidance of Central Nervous System Axons after Spinal Cord Injury

Permalink

https://escholarship.org/uc/item/3f860764

Author

Steinke, Christopher

Publication Date

2016

Peer reviewed|Thesis/dissertation

eScholarship.org Powered by the California Digital Library
University of California

UNIVERSITY OF CALIFORNIA, SAN DIEGO

Exploring Drug-Inducible BDNF in Promoting Regeneration and Guidance of Central Nervous System Axons after Spinal Cord Injury

A Thesis submitted in partial satisfaction of the requirements for the degree

Master of Science

in

Biology

by

Christopher Luke Steinke

Committee in charge:

Professor Daniel Gibbs, Chair
Professor Yishi Jin, Co-Chair
Professor Kathleen French

2016

The thesis of Christopher Steinke is approved, and it is acceptable in quality and form for publication on microfilm and electronically:

_____

_____

Co-Chair

_____

Chair

University of California, San Diego

2016

Dedication

I want to thank Dr. Daniel Gibbs for supporting me in my project, academic and personal development these last few years. While I have never seen myself as a writer, he makes it look easy and is an inspiration for academic writing. Lastly, to my dog: who sat and watched me type my entire thesis with only a little complaining.

Table of Contents

List of Figures

List of Tables

Acknowledgments

A tremendous thank you to Dan Gibbs and everyone at the Tuszynski lab for teaching me everything I know about hands-on biological techniques, research analysis and neuroscience in general.

Abstract of the Thesis

Exploring Drug-Inducible BDNF in Promoting Regeneration and Guidance of Central Nervous System Axons after Spinal Cord Injury

by

Christopher Luke Steinke

Master of Science in Biology

University of California, San Diego, 2016

Professor Daniel Gibbs, Chair
Professor Yishi Jin, Co-Chair

Spinal cord injury (SCI) affects upwards of one million people in the U.S. alone each year, with high costs to standards of living and healthcare (NSCISC 2015, #8). Present therapy targets increasing motor function and coping with medical complications though extensive rehabilitation. However, recovery remains difficult and restricted in scope for many, revealing the need for more therapeutic SCI development. Current research conceptualizes that a “neuronal relay” can be formed to bridge injuries of the

central nervous system in order to communicate motor and sensory signals that may perhaps aid recovery. Recently, Lu *et al.* 2012 showed that NSCs (Neural Stem Cells) have the potential for implantation, integration and synapse formation with host neurons over long distances when combined with growth factor cocktail and an extracellular matrix (Lu *et al.* 2012, #34). We theorize that signal cues are essential for guidance and synaptogenesis for growing axons from developing neurons, and Mai *et al* 2009 demonstrates that bound BDNF gradients in *in vitro* are involved in axon guidance (Mai *et al*. 2009, #36).

BDNF (brain-derived neurotrophic factor) is an important cue for neural development (Chen *et al.* 2007, #9) and synapse formation that has previously been investigated in the spinal cord by Park *et al.* (Park *et al.* 2013, #42). We propose two gene therapy techniques to over-express BDNF in specific neural populations in a drug-inducible manner for improvement of functional recovery. Transient, drug inducible expression of BDNF is essential to mitigate detrimental effects such as spasticity and neuropathic pain, which stem from constitutive overexpression of BDNF within the spinal cord (Fouad *et al*. 2013, #16). In Chapters 2 and 3 we show GsDREADD (Designer Receptor Exclusively Activated by Designer Drug) activation of the intracellular cAMP pathway by the artificial ligand CNO (clozapine-n-oxide) leads to strong expression of BDNF (Farrell *et al.* 2013, #15). *In vitro* examination of GsDREADD signaling in primary neuronal culture reveals its efficacy for regulated BDNF expression (Chapter 2) in a drug-dependent manner. *In vivo* implementation of GsDREADD through AAV transduction into the spinal cord displays strong BDNF production local to the site of injection, but appears to be activated regardless of drug-withdrawal (Chapter 3). Lastly, an alternate method for drug-inducible BDNF production was pursued through “DD-BDNF” technique, which utilizes the degradation domain (“DD”) of bacterial dihydrofolate

reductase enzyme (DHFR) fused to the proBDNF N-terminal, The destabilizing DD tag prompts rapid and efficient cellular degradation of the fused protein—proBDNF—via the proteasome before it can be fully expressed. DD-constructs are stabilized in the presence of the FDA approved antibiotic drug TMP (Trimethoprim) to allow temporal regulation of gene expression in a drug-dependent manner. A recent report from the Maximov lab (Sando *et al.* 2013, #49) demonstrated the feasibility of using this "DD" approach to control the expression and activity of Cre recombinase, EGFP or synaptic proteins in the CNS of transgenic animals and in animals treated with viral vectors expressing DD-constructs. Chapter 4 focuses on *in vitro* pursuit of DD-BDNF as a viable alternative to GsDREADD for driving drug inducible BDNF expression. Thus far, we have preliminary data demonstrating successful drug inducible control of exogenous BDNF protein expression using DD-BDNF and TMP *in vitro.* We are currently repeating this to verify our results. We seek to identify a time course and dose response profile of TMP dependent DD-BDNF induction prior to *in vivo* testing and following completion of AAV-CAG-gCOMET-DD-BDNF vector production.

Chapter 1: Introduction

The mammalian central nervous system does not regenerate because of growth-inhibitory intrinsic and extrinsic factors (Kaplan *et al*. 2015, #25), such as the formation of a glial scar (Sofroniew *et al*. 2005, #51), myelin-associated inhibitors (Akbik *et al.* 2012 #1, Geoffroy *et al.* 2014 #12), axon debris, and the limited regenerative capacity for adult CNS axons (Lu *et al*. 2007, #29). Recent success has been found with replacing injured adult neurons of the CNS with embryonic Neural Stem Cells (NSCs) that are not intrinsically inhibited and have the potential to grow axons long distances after implantation in the injured spinal cord (Lu *et al*. 2012, #34). Limited by the ability of adult CNS axon regeneration, our proposed treatment to spinal cord injury is implantation of NSCs to form a neural "relay" that would facilitate signals passing through the injury site onto their original targets—in order to promote recovery for both sensory and motor functions. However, while NSCs show great growth potential, they do not synapse upon the appropriate targets or integrate well with host neurons (Lu *et al*. 2012, #34). Incorrect synaptic development should be avoided because it can lead to aberrant connections, such as those causing spasticity and neuropathic pain (Fouad *et al*. 2013, #16)

In this thesis I propose and develop two methods by which growing NPC axons can be guided to their appropriate targets in order to correctly relay host sensory and motor signals. I put forward BDNF (Brain-Derived Neurotrophic Factor) as a robust and appropriate signal to guide developing axons (Xu *et al*. 1995 #61, Song *et al*. 1997 #52, Mai *et al*. 2009 #36). To achieve transient and localized BDNF expression, I developed two different plasmids (Table 1) that induce BDNF and are chemically controlled. Our research question is as follows: does localized drug-induction of BDNF offer appropriate signaling for developing NSCs that can be used to orient and guide them towards suitable host neural circuits and limit adverse side effects.

First, I developed and created two different BDNF-inducing techniques that are drug-inducible (Chapter 2). Next, I address aim 1: *in vitro* verification of plasmids in cell lines or primary cell culture through AAV transduction (Chapter 2). Following; I addressed aim 2: *in vivo* AAV injection and transduction of uninjured Fischer rat spinal cord to verify temporal and spatial localization (Chapter 3). Aim 3—verification of BDNF-associated axon guidance in T4 complete transection in Fischer rats as an applicable model of spinal cord injury—was not followed because of challenges identified in aim 2; *in vivo* validation. Instead, I developed an alternate drug-inducible BDNF technique that addresses *in vitro* validation and is currently moving into *in vivo* confirmation following final AAV production (Chapter 4). By the conclusion of this Master's thesis, I show that BDNF production can be drug-induced *in vitro* and regulated in a spatially constrained manner *in vivo*.

Chapter 2.1: Introduction to GsDREADD approach

The DREADD system (Designer Receptor Exclusively Activated by Designer Drug) is a technique for drug-dependent regulation of intracellular signaling. Specifically, GsDREADD is a GPCR (G-protein coupled receptor) made from recombinant muscarinic receptor that is only activated by the artificial ligand CNO (clozapine-n-oxide)—a ligand that is otherwise inert (Farrell *et al*. 2013, #15). CNO activation of GsDREADD cause guanine exchange of the Gas subunit, replacing GDP with GTP and initiating second messenger signaling cascade of the cAMP pathway. cAMP directly regulates PKA (protein kinase A) activity, causing phosphorylation of downstream transcription factors such as CREB (Siddiq and Hannila *et al.* 2008, #50).

Phosphorylated CREB has been shown to increase BDNF expression (Melemedjian *et al*. 2014, #38). Regulation of intracellular cAMP levels affects many transcriptional factors, all of which have not been identified. Nonetheless, therapeutic elevation of cAMP levels has been shown to be beneficial to neuronal health and differentiation (Blesch *et al*. 2012, #3) and to enhance axon regeneration (Ghosh-Roy *et al.* 2010 #19, Hellstrom *et al.* 2014 #22). Therefore we concluded that although GsDREADD activation is expected to cause unknown effects beyond BDNF axon guidance, cAMP side effects are generally beneficial to cell grafts and de-innervated host tissue and fall within the scope of promoting cellular growth (Hannila *et al.* 2008, #50). Lastly, CNO removal should be a reliable method to cease any GsDREADD effects both *in vitro* and *in vivo*.

Adverse side effects such as spasticity can be avoided by limiting when BDNF is drug-induced as well as targeting only a spatially restricted area of spinal cord. We developed two AAV plasmids, p976 and p1112 in Table 1, which co-express

GsDREADD and either GFP- or RFP-based enhanced fluorescent reporters (COMET vectors, developed in the Gibbs lab) respectively. Adeno-associated viral vectors were made with two different serotypes: AAV8 to maximize spread and infectivity, or AAV2 to limit vector spread and spatially restrict GsDREADD expression for induction of a localized BDNF gradient. We hypothesize that spatial restriction of GsDREADD expression, and by extension BDNF production, will be important for the formation of neurotrophic gradients capable of guiding growing graft derived axons to appropriate synaptic targets; for example – to lower motor neuron pools in ventral grey matter below the level of the lesion and graft. Embryonic (E18) rat cortical cultures were used as an *in vitro* model of the nervous system for GsDREADD plasmid electroporation or AAV transduction. CNO drug time points were selected to maximize detection of intracellular signaling: 0, 0.5, 1, 2, 6, and 24 hours post-CNO application. BDNF ELISA was implemented to analyze secreted BDNF in the cell supernatant. Cells were harvested and lysed for Western blotting to analyze intracellular protein expression levels and phosphorylation levels of downstream signaling molecules: e.g. proBDNF, P-CREB, and P-ERK.

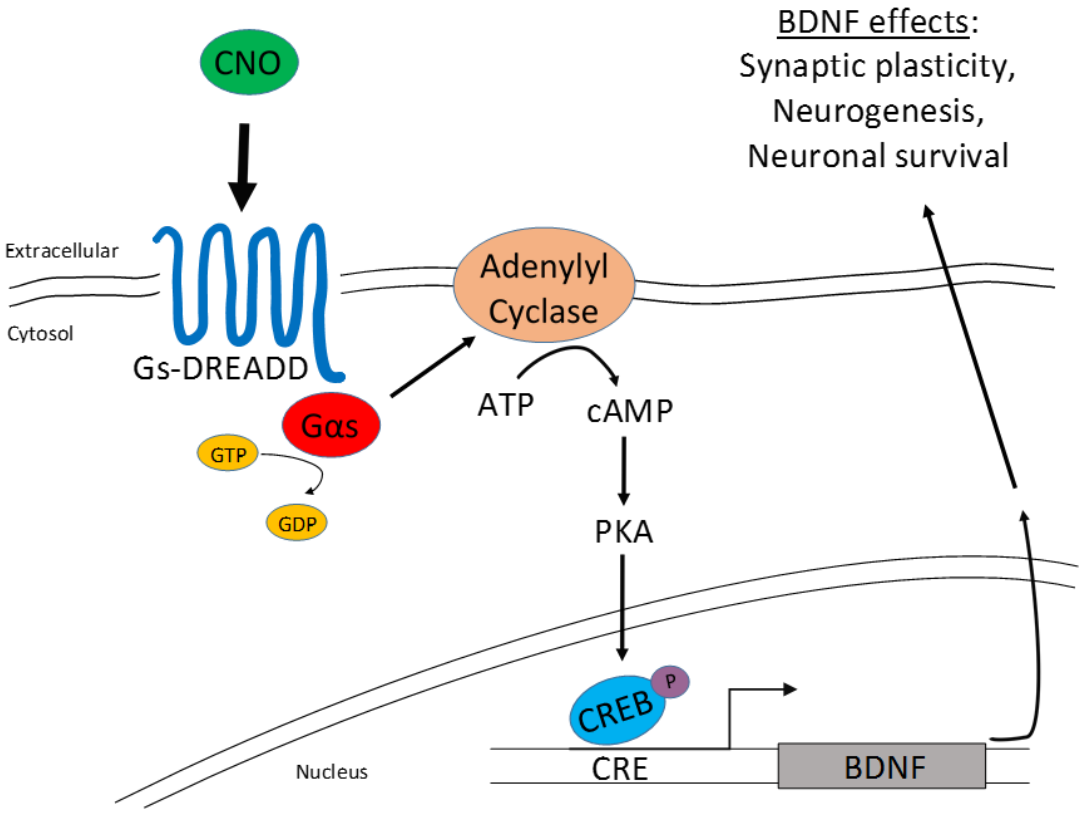

Figure 1: Simplified GsDREADD pathway to show the activation of GsDREADD by CNO leading to cAMP elevation, CREB phosphorylation and BDNF expression.

Chapter 2.2: GsDREADD *in vitro* Materials and Methods

Development of GsDREADD-expressing plasmids: p976, p1112

All plasmids used were derived from in-house Tuszynski laboratory plasmid backbones using In-Fusion cloning to insert PCR fragments of genes of interest (ClonTech #011614). After development, all four plasmids were transformed into NEB5α competent cells (NEB, C2987H), plated on LB-agar plates, and incubated at 37◦C overnight. Colonies were picked and grown up overnight again in S.O.C. medium (ThermoFisher 15544-034). DNA from picked colonies was isolated with the Qiagen Spin Miniprep Kit (Qiagen, 27106) and the DNA sequences were then confirmed using selective restriction digest and Sanger sequencing (Eton Sequencing). Verified colonies containing the desired plasmids were scaled up by growing at 37◦C overnight in TB medium with antibiotic, and then isolated with the Qiagen EndoFree Plasmid maxiprep kit (Qiagen, 12391).

Plasmid p976: pAAV-CAG-gCOMET-GsDREADD was derived from the plasmid backbone p833: pAAV-CAG-gCOMET-H2B:mCherry with the GsDREADD gene inserted through In-Fusion cloning at the compatible NheI—NotI site, replacing the H2B:mCHerry cDNA. The incorporation of “2A-like” sequences allows co-expression of gCOMET with another cDNA downstream on the in-frame T2A skip sequence (Donnelly *et al.* 2001, #14). The associated GsDREADD gene was PCR-amplified from the plasmid pAAV-Ck1.3-Ha-GsDREADD-IRES; mCitrine (Roth *et al.* 2011 #15). Plasmid 1112: pAAV-CAG-rCOMET-GsDREADD was made similarly but as a red variant of plasmid p976. The same PCR-amplified GsDREADD was inserted through In-Fusion Cloning into the backbone p1055: pAAV-CAG-rCOMET at similar NheI—NotI sites.

GsDREADD AAV Production

Plasmids 976 and p1112 were separately packaged into Adeno-Associated Virus (AAV) at the Salk Institute GT3 core in La Jolla. Plasmid p976 was packaged into both AAV8 and AAV2 serotypes. AAV8 was chosen because it has been shown to diffuse extensively in the CNS, and also is actively transported along axons (Castle *et al.* 2014, #7) AAV8 vectors were chosen for widespread expression of GsDREADD, to initially assess efficacy of CNO-mediated stimulation of endogenous BDNF production. AAV2 binds to heparin sulphate proteoglycans (HSPGs) in the ECM (Nicklin *et al.* 2001, #14), and demonstrates much more restricted spread in the CNs compared to AAV8. AAV2 was chosen to limit the spread of transduction in order to spatially restrict the amount of transduced spinal cord tissue to a defined anatomical region. Plasmid p1112 was similarly packaged into AAV2 for limited viral spread in the spinal cord. Viral titers can be found in Table 1.

Embryonic Cortical Culture Extraction, Transduction or Electroporation, and Culturing

Pregnant Fischer F344 dams with offspring of embryonic day 18 (E18) were anesthetized with an overdose IP injection of ketamine/ acepromazine/ xylazine and then sacrificed. Cortices of E18 embryos were harvested and dissociated as described in the Lonza Amaxa 4D-Nucleofector Protocol for Rat Hippocampal and Cortical Neurons (BioResearch 2012, #2). In some experiments, cortical neurons were plated without electroporation and transduced with the appropriate AAV with an MOI of 5×10^3. If the experiment did not call for viral transduction, neural cells were instead electroporated with the specific plasmid associated with that experiment. All rat cortical cultures were plated on PDL-coated 6- or 12-well plates at a density of 5 or 2.5×10^6 cells, respectively. Two days after plating, non-electroporated neuronal cultures were evaluated for vitality and then followed up with AAV transduction.

BDNF ELISA of Cell Supernatants

Secreted BDNF in cell media was quantified using the R&D Systems Human Free BDNF Quantikine ELISA kit (R&D DBD00). Methods were performed as described in the included protocol, with appropriate calibration curve to determine BDNF present.

Western Blots of Cell Lysates

Cell lysate BDNF was determined by Western blot following the ThermoFisher NuPage Western blot technical manual (NuPage IM-1001, pg. 35-53) and using Precision Plus Protein All Blue Prestained Protein Standards (Bio-Rad #1610373). Antibody's used and their appropriate dilutions can be found in Table 2.

Chapter 2.3: GsDREADD *in vitro* Results

To validate BDNF production in embryonic cortical culture, we analyzed BDNF secreted into the cell media by BDNF ELISA over a time-course of CNO administration. BDNF and CNO are stable at 37°C for longer than 24 hours, and so we expect BDNF to accumulate with longer exposures to CNO. Figure 2.1 below shows BDNF secretion from cortical cells.

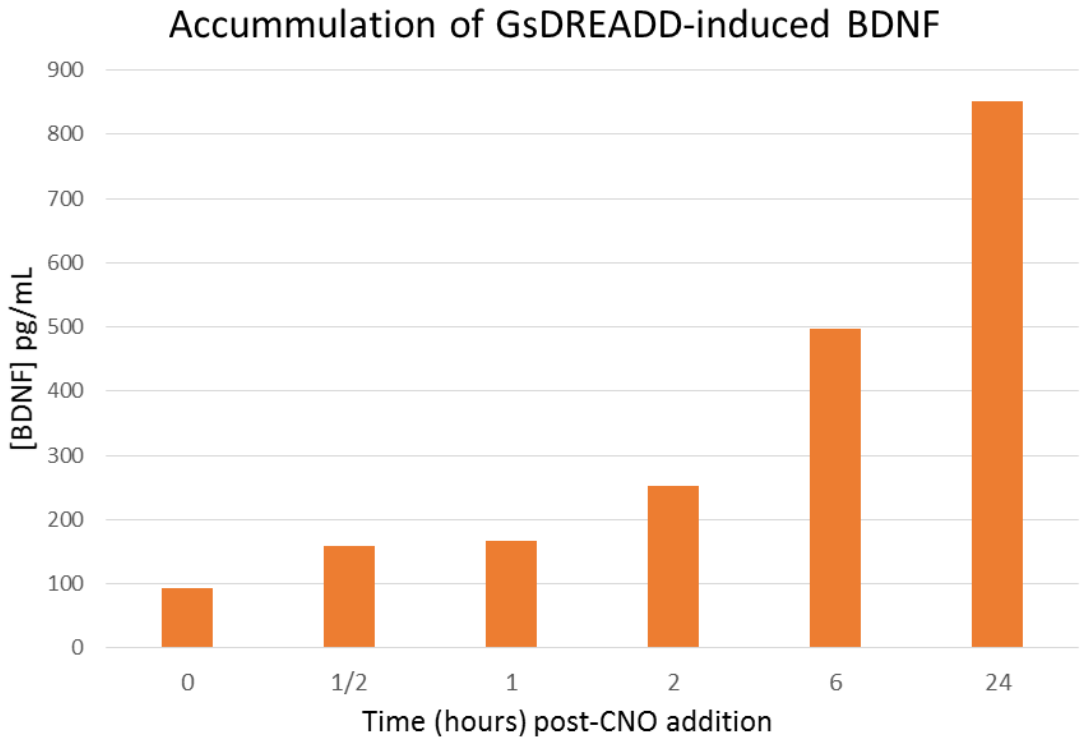

Figure 2.1: BDNF ELISA of GsDREADD-transducted embryonic cortical culture supernatants following CNO time course

Additionally I investigated intracellular signaling events downstream of the GsDREADD receptor and production of the proBDNF protein following CNO activation to validate GsDREADD activity through Western blot of cortical culture cell lysates. proBDNF was probed in two different cell cultures to indicate the drug-dependent timecourse *in vitro*. Cell culture one was transfected with AAV8-CAG-gCOMET-

GsDREADD at 10^4 MOI, and cell culture two was transfected with AAV2-CAG-gCOMET-GsDREADD at 5 x 10^3 MOI because of lower viral titer. Figure 2.2 shows the two cell cultures' proBDNF expression.

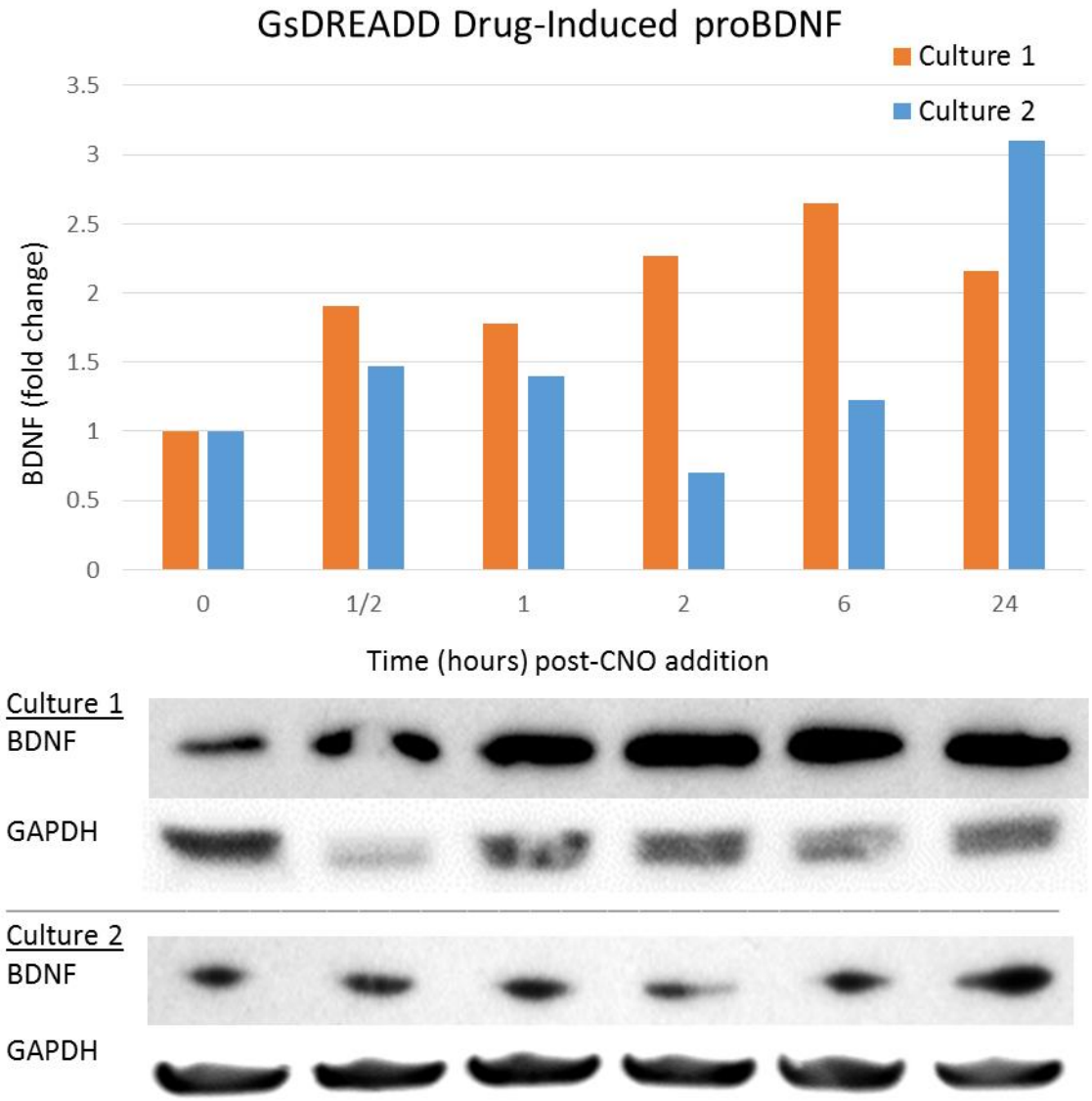

Figure 2.2: proBDNF Western of AAV2 and AAV8 GsDREADD-transducted embryonic cortical culture lysates following CNO timecourse

To investigate a mediator of intracellular signaling downstream of GsDREADD receptor activation, and upstream of BDNF transcription; I chose to probe culture 2—transfected byAAV2-CAG-gCOMET-GsDREADD—for Phosphorylated CREB (P-CREB) via Western blot. CREB is activated by phosphorylation at serine 133—via PKA in response to elevated cAMP. P-CREB (ser133) binds to CREB response elements (CRE) in many immediate early genes involved in growth and neuroprotection, including BDNF, and initiates transcription.

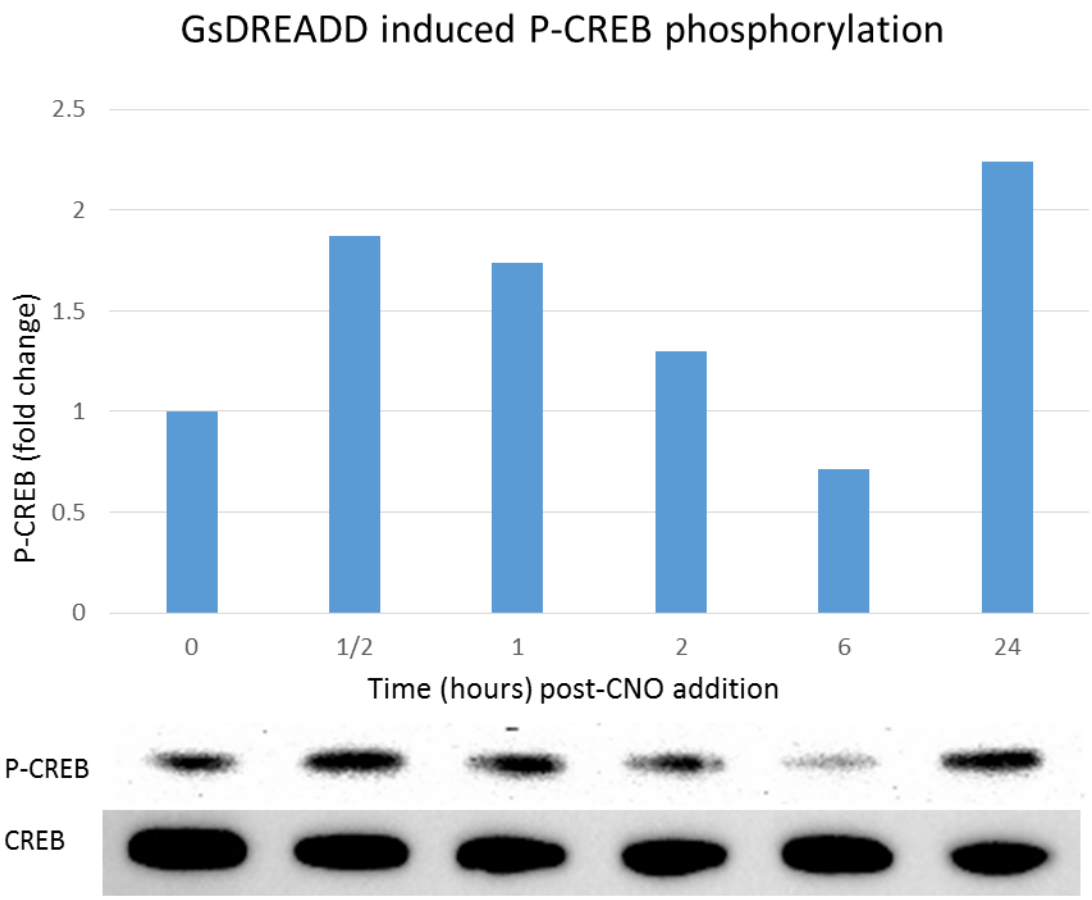

Figure 2.3: Phospho-CREB Western blot of AAV2-CAG-gCOMET-GsDREADD transducted embryonic cortical culture lysates following CNO timecourse

Exploring autocrine BDNF activation of its cellular receptor, TrkB, led me to probe activation of the MAPK (mitogen activated protein kinase) pathway downstream of the TrkB receptor, that has been so extensively studied for its growth stimulating effects. Figure 2.4 below shows ERK (also known as MAPK) phosphorylation (P-ERK Thr202/Tyr204).

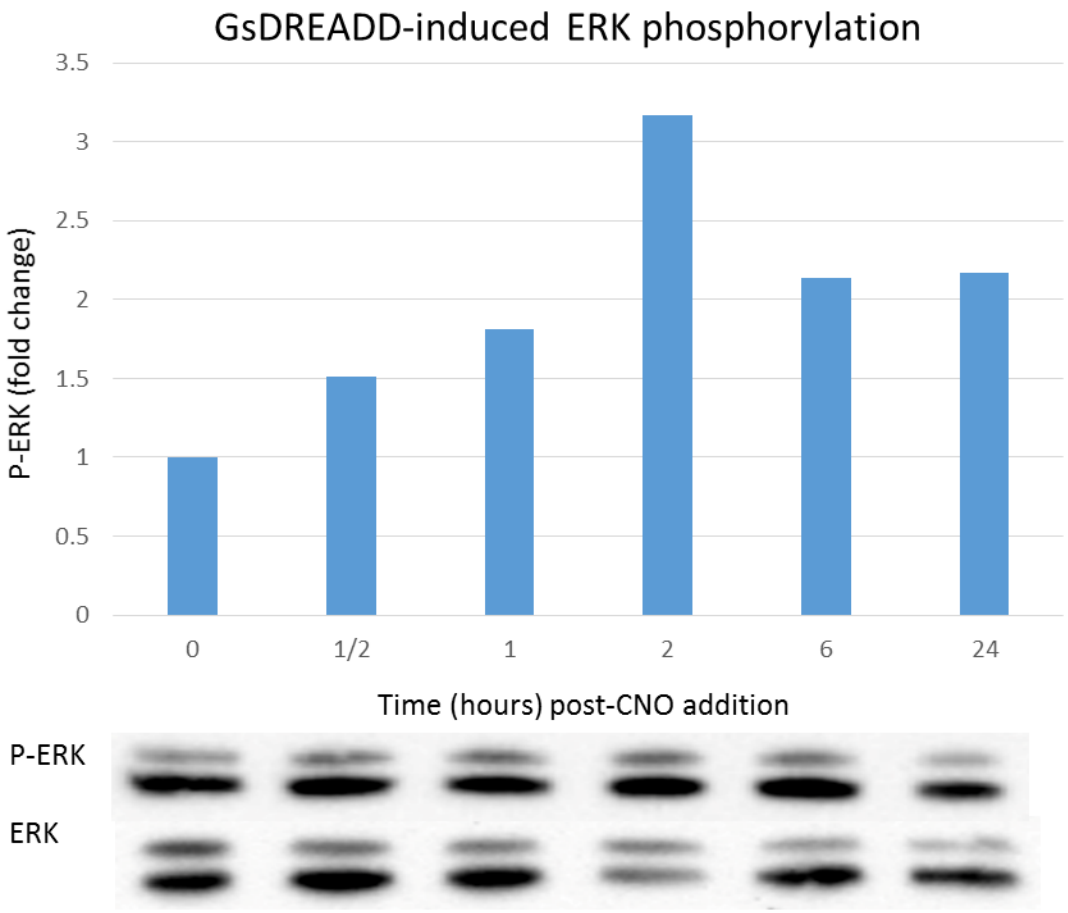

Figure 2.4: Phospho-ERK Western of AAV2-CAG-gCOMET-GsDREADD transducted embryonic cortical culture lysates following CNO timecourse

As a third method of *in vitro* validation of GsDREADD in embryonic cortical culture, I cultivated and transfected a third rat embryonic cortical culture with AAV2-

CAG-gCOMET-GsDREADD. After 14 DIV, cultures were treated with CNO and individual wells were sampled at specific time points after drug administration to analyze BDNF expression by immunocytochemistry. Cells were fixed with 0.2% PBQ, 2% PFA solution, and immunostained for BDNF at respective CNO time points seen in Figure 2.5. These images are representative of the culture as a whole, where increased BDNF staining appears to correlate to longer dosage of CNO.

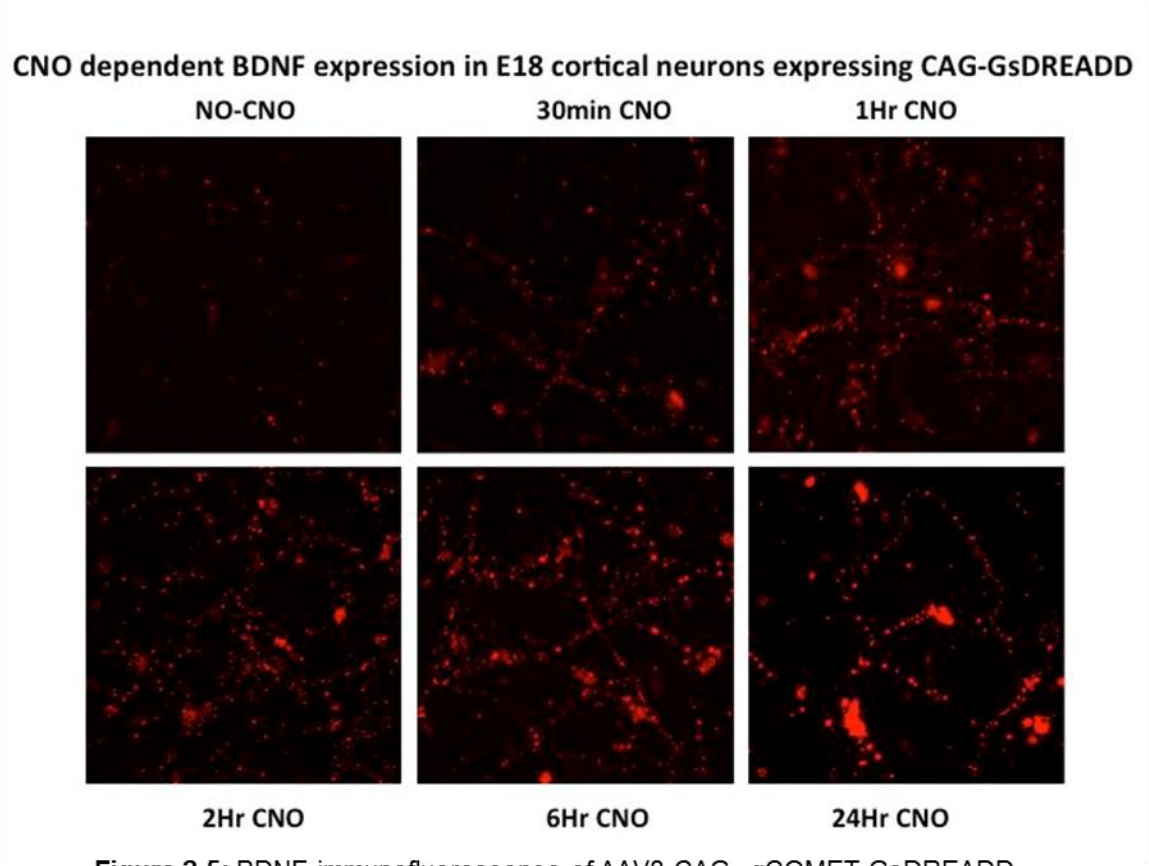

Figure 2.5: BDNF immunofluorescence of AAV8-CAG- gCOMET-GsDREADD transducted embryonic cortical culture with following CNO timecourse

Chapter 2.4: GsDREADD *in vitro* Discussion and Future Directions

The GsDREADD system appears to show drug-regulatable properties that result in elevated BDNF expression when expressed through an AAV vector delivery. Figures 2.1 BDNF ELISA, Figure 2.2 proBDNF Western, and Figure 2.5 BDNF immunostaining are independent approaches to measuring BDNF levels *in vitro*. BDNF ELISA (Figure 2.1) shows increased BDNF accumulation in cortical culture cell media over 24 hours, demonstrating that drug induced activation of GsDREADD resulting in BDNF expression continues in the presence of CNO for at least 4 hours *in vitro* and potentially longer. Even though BDNF can bind to TrkB receptors and is internalized for TrkB signaling, BDNF is relatively stable in cell media and should not be degraded in significant quantities over the experimental time frame.

ProBDNF (Figure 2.2) and P-CREB (Figure 2.3) are from different biological replicates and appear to be elevated following CNO administration. Interestingly, they both follow a biphasic pattern of increased immediate expression within the first hour, followed by return to normal expression levels, and lastly strong activation around the 24 hour time point. GsDREADD activation could be biphasic for the time frame studied because of receptor internalization and desensitization in response to cAMP pathway overstimulation. However, more replicates and additional neuronal cell types must be investigated to determine biphasic properties and to replicate of each experiment for repeatability. Figure 2.4 demonstrates Western blot of ERK phosphorylation, as a read-out of TrkB signaling in response to BDNF or receptor cross-talk. Intracellular P-ERK is a regulator of the MAPK pathway that is also involved in neurogenesis and axonal growth.

A separate culture of embryonic cortical neurons was cultivated on coverslips, given the same CNO treatment timeframes, and fixed for BDNF immunostaining. Figure

2.5 shows a significant increase in BDNF immunoreactivity over time in response to CNO administration, both in the intensity of BDNF staining and in the size of the BDNF positive puncta. These results when taken together, independently confirm that CNO dependent activation of ectopically expressed GsDREADD leads to significant stimulation of endogenous BDNF production. While addition replicates need to be completed, the BDNF immunostaining is promising as a parallel study because it also implies the same conclusion through independent experimentation. In conclusion, drug-activation of BDNF through the CNO-GsDREADD system is a viable method of controlling endogenous BDNF expression *in vitro* and should be expanded through AAV mediated *in vivo* BDNF expression studies. Chapter 3 builds upon these *in vitro* studies and applies the GsDREADD system to *in vivo* rat models of spinal cord utilizing an AAV-mediated gene therapy approach.

Chapter 3.1: GsDREADD *in vivo* Introduction

Chapter 2 demonstrates that the GsDREADD system is a valid method for driving endogenous BDNF expression in cultured primary embryonic neurons *in vitro*. However, to develop the CNO-GsDREADD method as a clinically applicable tool, it needs to be capable of inducing endogenous BDNF expression in a drug-dependent manner *in vivo*, and at levels of expression that would be expected to be biologically active. Ideally, CNO administration should elevate BDNF protein levels significantly above basal levels, while CNO withdrawal should halt GsDREADD signaling and bring BDNF protein levels back down to baseline without significant delay. Chapter 3 addresses aim 2: verification of GsDREADD *in vivo* using AAV injections into uninjured Fischer rat spinal cord. This model was chosen because it is used extensively in Lu *et al.* 2012 and our group as a well-established animal model of thoracic and cervical SCI. Additionally, I plan to use this model for BDNF guidance studies under a similar paradigm. To make my results consistent between models of uninjured and injury spinal cord, I will be using the same species and similar location within the spinal cord for AAV injections in both the uninjured and injured spinal cord. With a localized and drug-inducible BDNF expression system, I hope to guide axons from a Neural Stem Cell (NSC) graft for optimized integration with host neuronal circuits below the level of the injury.

Two different vector systems were optimized for *in vivo* experiments: AAV8 for widespread infectivity under different cell types, and AAV2 for localized infectivity. First, AAV spread in the uninjured cord was characterized by immunostaining spinal cord sections for either gCOMET or rCOMET reporters to allow characterization of AAV infectivity and GsDREADD expression levels. Second, I analyzed GsDREADD

stimulation in the transduced cord through light level immunohistochemical staining of BDNF. Simplified CNO dosing time points similar to those in *in vitro* studies were used in order to qualitatively determine BDNF expression with and without CNO. It's important that the drug inducible levels of endogenous BDNF protein be high enough to form a functional neurotrophic gradient for stimulation of axon growth and guidance from the neural stem cell graft when stimulated by CNO. It is also essential that GsDREADD is drug-regulated *in vivo* otherwise constitutive BDNF secretion can cause side effects such as spasticity and neuropathic pain.

Chapter 3.2: GsDREADD *in vivo* Materials and Methods

Animal Protocols

Adult female Fischer 344 rats 150-200g were studied. Animals had constant access to food and water throughout the study, and all animals were deeply anesthetized using a 2ml/kg cocktail of ketamine (25mg/ml), acepromazine (0.25mg/ml) and xylazine (1.3gm/ml). Guidelines for laboratory animal care and safety were followed in accordance with NIH.

AAV C8 Dorsal Column Injections

Adult Fischer 344 female rats were anesthetized by IP injection of ketamine/ acepromazine/ xylazine cocktail. A glass-pulled capillary tube with Pico-spritzer attachment was loaded with 2ul of appropriate AAV. The subject was mounted into a rat stereotax by ear bars and curved hemostatic forceps clamped the T2 projection to hold the spinal cord immobile. The subject was opened with a scalpel and retractors (Roboz RS-6500) until the cervical C4-C8 spinal cord segments were visible. A small hole in the dura was made by fine tip forceps (Dumont #3) to alleviate CSF pressure. The glass-pulled capillary injector was then inserted into the spinal cord between the C6-C7 vertebrae (C8 spinal level) 0.8mm left of midline and at a depth of 2.0mm. 1.0ul of AAV was injected by picospritzer at a rate of 0.5ul/minute into the ventral horn. The capillary injector then was raised 0.5mm and 1.0ul of AAV was injected into the dorsal horn at the same rate. After waiting 10 seconds to reduce reflux, the capillary and retractors were removed and the wound was sutured. Neo-Predef antibiotic powder was applied to the wound, wound clips joined the skin together, and the rat was given a subcutaneous injection of banamine, ampicillin, and lactated ringer's solution for 3 days post-surgery and placed on heat pads overnight. Wound clips were removed 10-14 days later.

Immunohistochemistry and Analysis

Perfused tissue from previously described experiments were post-fixed overnight in 4% PFA in 0.1M phosphate buffer at pH 7.2. Spinal cords and brains were dissected and placed in 30% sucrose as cryoprotection for 72 hours. 1.5cm blocks on spinal cord tissue centering on the injection were sectioned horizontally on a sliding microtome at 35um. A representative series of sagittal sections were immunohistochemically processed as described by Lu *et al.* 2003, #28. We evaluated BDNF levels and GFP spread throughout the cord in order to show the distribution of the virus and drug activation of the proteins encoded by the virus. BDNF staining underwent additional PFA/ PBQ antigen retrieval step as outlined in Nagahara *et al.* 2009 #40. GFP staining undertook a methanol antigen retrieval step also described in Lu *et al.* 2003, #28. Immunohistochemistry antibodies and their respective dilutions are listed in Table 3. After staining, sections were mounted on glass coverslides. Fluorescent-antibody stained section were dried overnight and then coverslipped with Fluoromount G (Southern Biotech 0100-01). Light-level stained sections were dehydrated and coverslipped with DPX mountant (Sigma-Aldrich 4581).

Scope Imaging and Quantification of Staining

Light level and fluorescent imaging was performed on a Keyence BZ-X710 scope with XY stitching. Images were taken on bright field or multiple fluorescent channels to allow image overlay and colocalization analysis. Thresholding light level images using ImageJ determined the area and intensity of light level staining to compare BDNF staining intensity between experimental conditions.

Intravitreal Injections of AAV or CTB

Adult Fischer 344 female rats were anesthetized by IP injection of ketamine/ acepromazine/ xylazine cocktail. A glass-pulled capillary tube was loaded with either 2ul of AAV or CTB. A small hole was made with a 25 gauge needle in the cornea at the edge of the lens with an angle into the vitreous humor. The glass-pulled capillary tube was then inserted into the vitreous humor and delivered either CTB or AAV by plunger. The glass capillary tube was removed after 10 seconds and neomycin, polymyxin, bacitracin-containing ophthalmic ointment was placed on the eyes for 2 days post-surgery. 3 weeks later, the rat was perfused with cold saline and then 4% PFA. Retinal tissue was carefully dissected and processed immunohistochemically for either GFP, beta-3-Tubulin, HA-tags, BDNF, or Brn3A.

Optic Nerve Crush

Adult Fischer 344 female rats were anesthetized by IP injection of ketamine/ acepromazine/ xylazine cocktail. Dumont #7 fine tip forceps, Jacobson microscissors, and Dumont #N7 cross-action forceps were used to open the caudal conjunctiva, rotate the eye, and spread the muscles and fatty tissue apart over the optic nerve. The cross action forceps were when used to crush the optic nerve for 10 seconds at 3mm from the back of the eye with a point 2mm from the tip of the fine forceps. Forceps were withdrawn and antibiotic eye ointment was delivered for 3 days post-surgery. 3 weeks later, the subject underwent CTB intravitreal injections. 2 days post-CTB injection, the animal was perfused with cold saline and 4% PFA.

Retinal and Optic Nerve Tissue Processing

Four weeks following AAV intravitreal injections, and two days post-CTB intravitreal injections, adult Fischer rats were anesthetized with an IP overdose ketamine/ acepromazine/ xylazine cocktail injection. The rat was then perfused with cold

saline followed by cold 4% PFA, and the head was removed by gross dissection and fixed overnight in 4% PFA. The following day, the retina and optic nerve were carefully dissected and placed into 30% sucrose as a cryoprotectant. Several days later, the retina was stained for Brn3A, beta-III-tubulin, or GFP and then flat mounted on a glass coverslip. Optic nerves were sectioned at 15um on a cryostat, directly mounted onto glass coverslides, and processed immunohistochemically for GFP or CTB tracing.

Chapter 3.3: GsDREADD *in vivo* Results

To determine AAV spread within the uninjured spinal cord, I injected both AAV8- and AAV2-CAG-gCOMET-GsDREADD (p976) at cervical column C8. AAV8 vector distribution as observed by anti-EGFP immunostaining was widespread. Neuronal cell bodies were typically restricted to the primary injection site, with extensive fiber labeling throughout the cervical cord. Area of anti-eGFP labeled cell bodies averaged 1.5mm from the two most densely labeled sagittal sections from all animals, while gCOMET labeled axons extended greater than 10mm rostral and caudal. This amount of spread was useful for assessing BDNF expression in response to CNO administration, but has too large of a spread in the spinal cord at 1.27 x 10^{12} titer (Figure 3.1A, B) to be useful for generating a localized neurotrophic gradient.

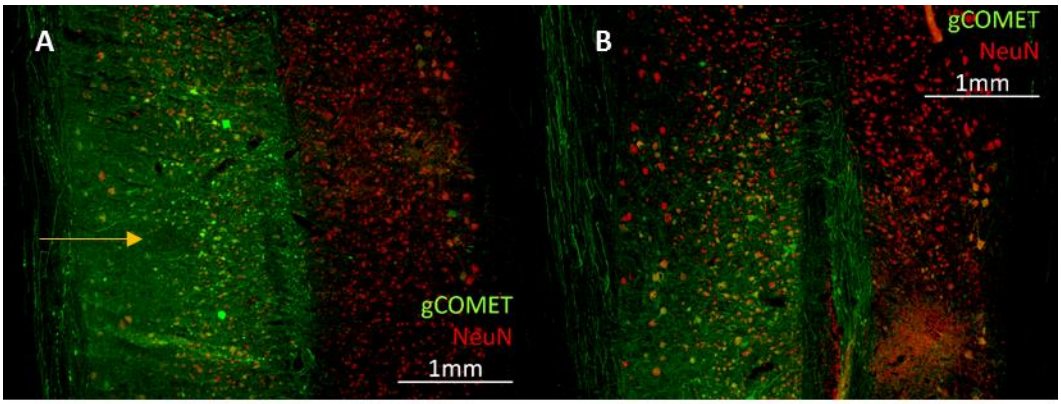

Figure 3.1: AAV8-CAG-gCOMET-GsDREADD (p976) immunofluorescence staining for gCOMET (green) and neuronal nuclei (NeuN: red). Panel A shows the area around the injection site (yellow) while panel B demonstrates long distance axon labeling and reporter spread.

To limit spread for optimal BDNF gradient localization, we repeated the experiment substituting AAV8 for AAV2-CAG-gCOMET-GsDREADD (Figure 3.2). Utilizing the gCOMET reporter as an indicator of transduced neurons, AAV8 appears to spread significantly more in the spinal cord while AAV2 is more localized to the injection

site. I also developed p1112 as a red reporter variant of p976 to allow for future co-localization studies of axon outgrowth and guidance from animals with SCI lesions engrafted with EGFP +ve neural stem cells, with AAV2-CAG-rCOMET:GsDREADD-transduced host neurons. Figure 3.3 shows a similar AAV2 spread to Figure 3.2, with clear neuronal nuclei and processes defined by rCOMET.

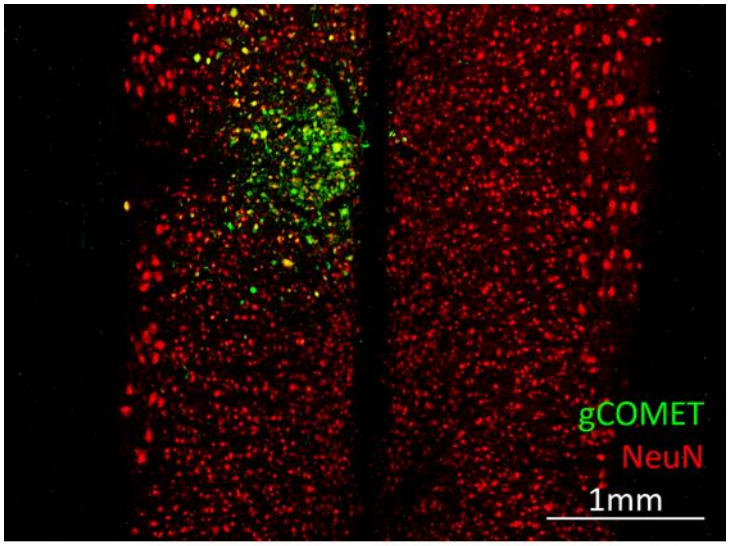

Figure 3.2: AAV2-CAG-gCOMET-GsDREADD (p976) immunofluorescence of transducted neurons and their

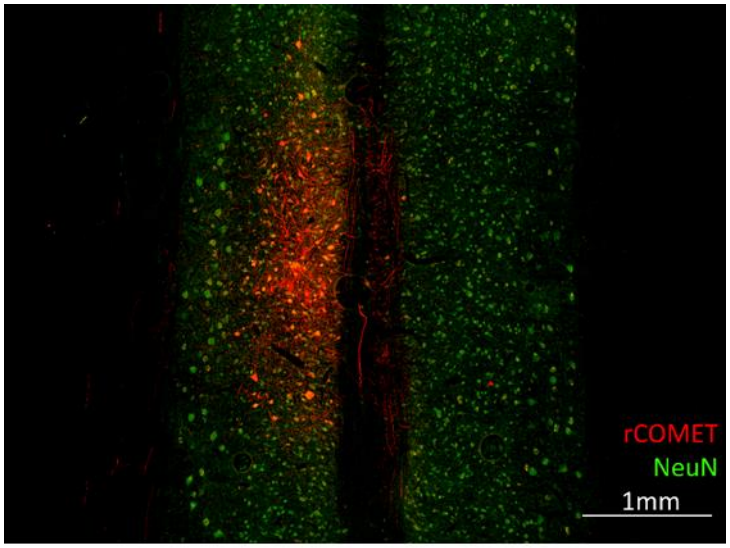

Figure 3.3: AAV2-CAG-rCOMET-GsDREADD (p1112) immunofluorescence showing transducted neurons and

Next I determined BDNF expression levels of the spinal cord sections shown in Figure 3.1 except following light level staining protocol for BDNF. AAV8-expressed GsDREADD in the presence of CNO appears to stimulate BDNF secretion widely throughout the cord with little localization around the injection site (Figure 3.4).

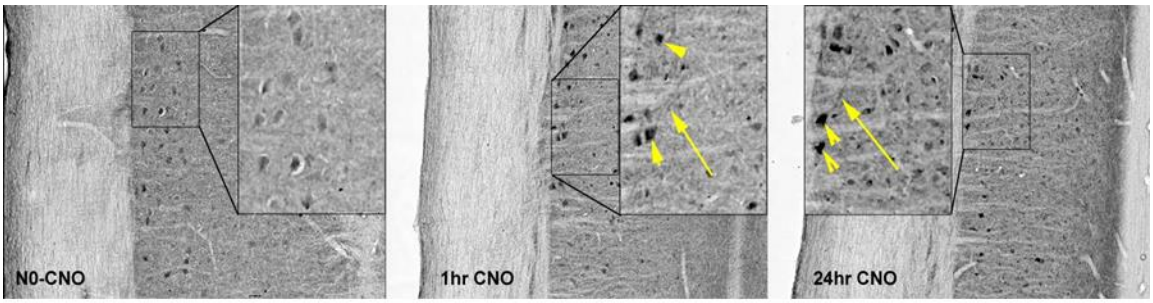

Figure 3.4: AAV8-CAG-gCOMET-GsDREADD (p976) light level BDNF staining around the injection site. "No CNO" (left) shows week cell body BDNF labeling, "1hr CNO" shows moderate cell body labeling with some defined projections, and "24hr CNO" (right) has the strongest BDNF labeling for cell bodies and neuronal processes. Arrow heads point to strong cell body labeling, while full arrows demonstrate labeled axons.

AAV2-expressed GsDREADD does allow BDNF spatial restriction around the injection site, which appears ideal for creating a neurotrophic gradient. While addition of CNO for 24 hours resulted in 2-3 fold increase in endogenous BDNF expression compared to the No CNO control—and a marked increase in BDNF compared to the contralateral grey matter that was uninjected—there appears to be elevated BDNF expression above basal levels around the AAV2-CAG-gCOMET-GsDREADD injection site in the absence of CNO (Figure 3.5).

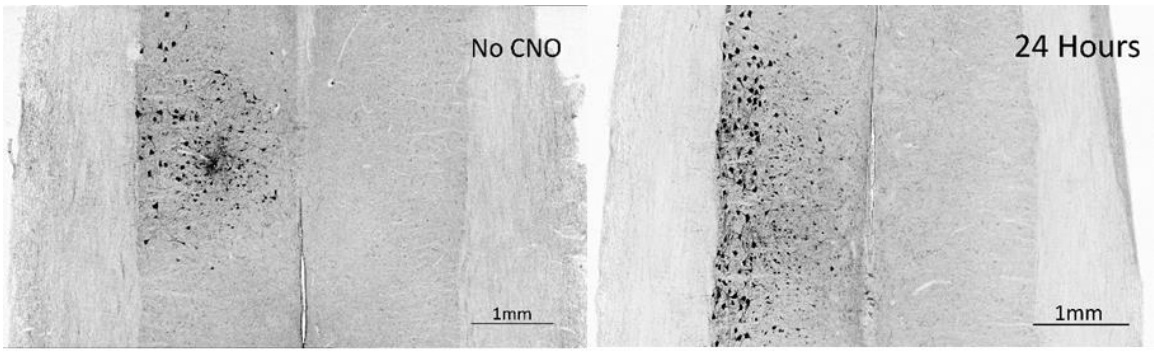

Figure 3.5: AAV2-CAG-gCOMET-GsDREADD (p976) light level BDNF. "No CNO" (left) shows BDNF immunostaining even without CNO administration, while "24 Hours CNO" (right) presents increased BDNF levels 24 hours post-CNO injection.

Lastly, I injected the constitutively active AAV2-CAG-BDNF as a positive control for BDNF overexpression, using the same surgical techniques and location as the GsDREADD AAV vectors. Sections were processed and stained for BDNF using the same light level protocol in order to verify BDNF immunohistochemistry techniques and AAV2 localization (Figure 3.6).

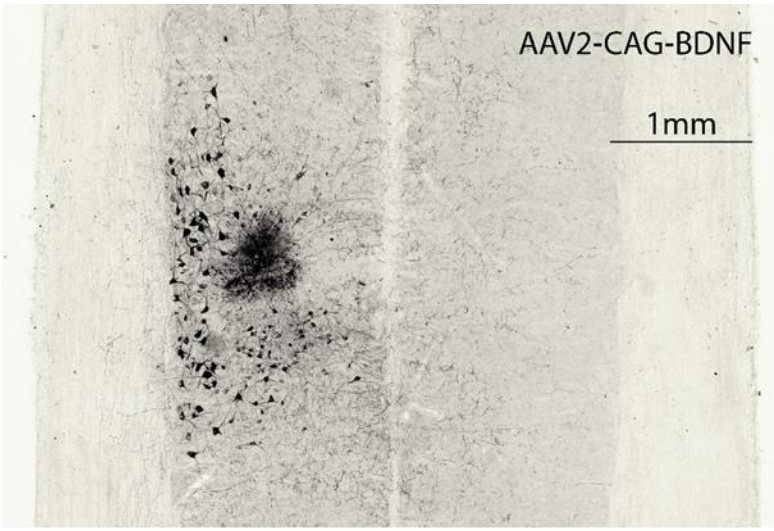

Figure 3.6: AAV2-CAG-BDNF injected uninjured spinal cord, light level immunohistochemically stained for BDNF.

BDNF staining intensity was quantified and compared in Figure 3.7 for multiple series of sections that all underwent PBQ antigen retrieval and light level immunohistochemistry for BDNF. Values are represented as the average and standard deviation of the three

most prominently BDNF stained sections for each group. ImageJ was used for threshold analysis of integrated density to compare all sections at the level given same microscope exposure settings.

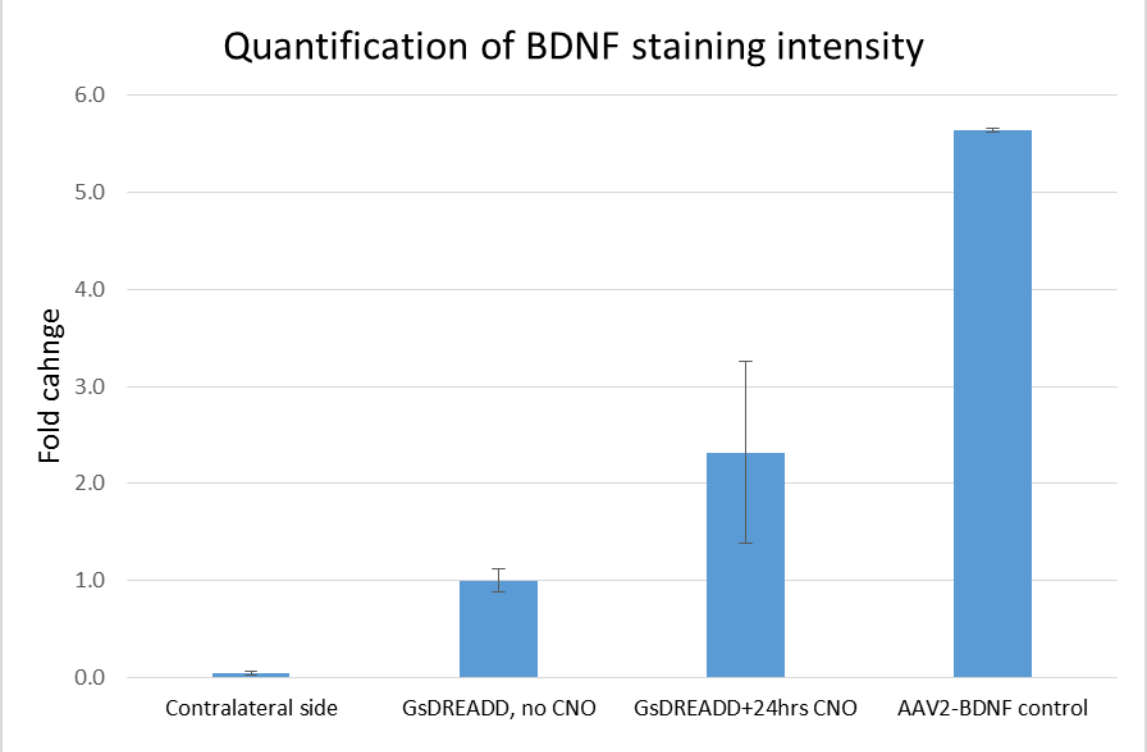

Figure 3.7: BDNF immunohistochemistry quantifcation using integrated density of 4 different groups: contralateral AAV2-BDNF, with and without systemic CNO (AAV2-CAG-gCOMET-GsDREADD), and AAV2-CAG-BDNF control. Staining was normalized to background BDNF labeling for all groups, with equal exposure.

Figure 3.8 shows the distribution of BDNF labeling following AAV2-injection. AAV2-GsDREADD with and without CNO, and AAV2-BDNF were all counted for number of positively BDNF labeled cell bodies. In combination with Figure 3.7, AAV2-BDNF shows a lower number of BDNF labeled cells, but a higher integrated density (strength of BDNF labeling) compared to AAV2-GsDREADD.

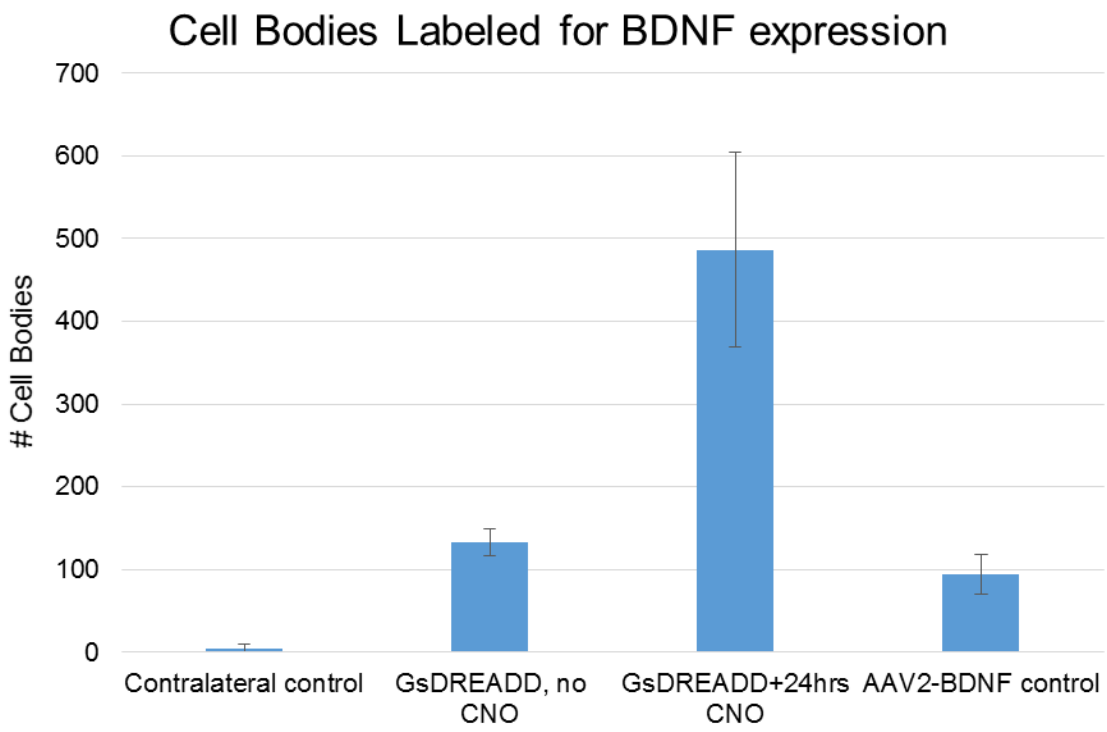

Figure 3.8: Number of BDNF-positive labeled cell bodies within 1mm of AAV2 injection site. Values are represented average number of counted cell, with error bars

In partaking with another project, AAV2-CAG-gCOMET-GsDREADD was also injected into the vitreous of the eye and combined with optic nerve crush in order to investigate optic nerve regeneration after crush injury. A limited set of GsDREADD-transduced optic nerves were measured and limited gCOMET labeling was found compared to CTB. Instead of optimizing optic nerve crush studies, I focused on spinal cord injury application of the GsDREADD system. Optic nerve sections have not been shown in this thesis.

Chapter 3.4: GsDREADD *in vivo* Discussion and Future Directions

I hypothesize that the GsDREADD system *in vivo* would allow elevation of endogenous BDNF expression similar to chapter 2 *in vitro* studies. Furthermore, regulated BDNF production *in vivo* is essential to enhancing integration and guidance of spinal cord grafts without adverse side effects, and could be assessed by using the Fischer rat model of spinal cord injury. I initially validated AAV-mediated expression of fluorescent reporter proteins, as well as the effect of AAV serotype on vector spread in order to determine the optimal method for GsDREADD vector delivery. Figure 3.1A, B and Figure 3.2 illustrate AAV8- and AAV2-CAG-gCOMET-GsDREADD expression, respectively. AAV8 transduces multiple cell types well and spreads across a large area of spinal cord around the injection site. I concluded that AAV8 is not ideal for localized BDNF delivery in the spinal cord, however it could have good potential for BDNF delivery in the brain for other neurodegenerative diseases, such as Alzheimer's (Nagahara 2009 #40). AAV2 transduces cells localized to the injection site and was selected for further studies in BDNF expression. Additionally, Figure 3.3 demonstrates the efficacy of AAV2-CAG-rCOMET-GsDREADD with similar transduction and spread as its gCOMET variant.

Figure 3.4 and 3.5 highlight BDNF expression (black) from anti-BDNF light level staining. These figures utilize a parallel set of spinal cord sections from Figures 3.1 and 3.2 to demonstrate BDNF spread relative to its gCOMET reporter. BDNF expressing cells seen by light level staining are well represented by gCOMET spread. Figure 3.5 also compares BDNF expression in GsDREADD transduced cells with and without CNO. There should be no BDNF staining above basal levels in cells expressing GsDREADD but without exposure to the ligand CNO. Instead, we detected BDNF expression above basal levels in the no CNO control (Figure 3.5A), which strongly suggests ligand-

independent activation of the GsDREADD. This could be potentially from the high levels of GsDREADD expressed within the cells under CAG promoter, or from injection of highly concentrated AAV2, leading to high copy number per cell, causing overexpression. However, addition of CNO does appear to activate GsDREADD *in vivo*, leading to strong overexpression of BDNF in the transduced area of spinal cord at levels that would be expected to be therapeutically relevant. In particular, the “24 hours CNO” condition (Figure 3.5) shows between 2-3 fold increased BDNF expression compared to the “No CNO” control, and much higher expression than the untreated contralateral grey matter (Figure 3.5). By comparison to animals treated with AAV2-CAG-BDNF (Figure 3.6), which drives constitutive overexpression of ectopic BDNF and is known to be potently neuroprotective (Nagahara 2009, #40), it is likely that the higher levels of BDNF seen in the “24 hours CNO” animals would be sufficient to generate a neurotrophic gradient capable of stimulating axon growth and guidance. Nonetheless, I determined that the CNO-GsDREADD system under these conditions (e.g. high local AAV concentration, strong cellular CAG promoter and moderate CNO doses) is not a reliable method for BDNF activation because the GsDREADD system *in vivo* appears “leaky” with elevated levels of BDNF in the “no CNO” control. One future direction would be to optimize AAV titers and test alternative promoters with weaker expression characteristics in an attempt to eliminate undesired ligand-independent activation. However, I pursued a promising alternative technique of drug-inducible BDNF. Rather than adopt an indirect method for driving elevated levels of endogenous BDNF, I investigated a new method for directly inducing expression of exogenously delivered BDNF in response to a systemically administered drug. This “DD-BDNF” method is explored in Chapter 4, beginning again with *in vitro* validation.

Chapter 4.1: Introduction to DD-BDNF

As an alternative to activating cellular signaling pathways to drive increased expression of endogenous BDNF in a drug dependent manner, I tested the feasibility of using exogenous expression of a drug inducible recombinant BDNF in place of upregulating endogenous expression through GsDREADD. This novel construct comprises full-length proBDNF cDNA fused to the degradation domain (“DD”) of the bacterial dihydrofolate reductase enzyme derived from Sando, 2013 #49. This construct is termed DD-BDNF. In the absence of the common antibiotic trimethoprim (TMP), the DD-BDNF protein should be rapidly degraded via the proteasome, leading to no detectable protein expression. Upon addition of TMP, the DD-BDNF protein should be rapidly stabilized, leading to rapid and reversible TMP-dependent BDNF protein overexpression (Sando, 2013 #49). 293TAB cells were transfected with DD-BDNF (N-terminal fusion) and BDNF-DD (C-terminal fusion) and analyzed to determine BDNF stability under drug conditions at periodic time points. Similar to GsDREADD, it is essential that BDNF be produced under drug-dependent conditions to avoid adverse effects during *in vivo* and therapeutic implementation.

Chapter 4.2: DD-BDNF Materials and Methods

Plasmid Development: p943 and p944

Plasmid p943: pAAV-CAG-BDNF:DD was originally derived from the in-house backbone p524: pAAV-CAG-BDNF. The destabilizing domain of the hDHFR gene sequence—which in theory should destabilize any connected protein—was amplified through PCR from the destabilized DD-CRE plasmid p1088: pAAV-CAG-rCOMET-DD:CRE (Sando, 2013 #49). The destabilizing domain sequence was then fused into the p524 plasmid at the N-terminal of the BDNF gene through In-Fusion cloning. Similar to p943, plasmid p944: pAAV-CAG-DD:BDNF was developed by inserting the DHFR's DD domain into the p524 backbone, but instead using In-Fusion cloning to fuse the "DD" to the C-terminal of the BDNF gene. After fragment insertion and ligation, plasmids were transformed into NEB5α competent cells (NEB, C2987H), plated on LB-agar plates, and incubated at 37°C overnight. DNA from picked colonies was isolated with the Qiagen Spin Miniprep Kit (Qiagen, 27106) and the DNA sequences were confirmed using services from Eton Sequencing. Picked colonies of verified plasmids were scaled up in volume and concentration by being grown at 37°C overnight in TB with antibiotic, and isolated by the Qiagen EndoFree Plasmid kit (Qiagen, 12391).

Virus Development and Production

Plasmids p944 is being custom packaged into Adeno-Associated Virus (AAV) at the Salk Institute GT3 core in La Jolla. p944 pAAV-CAG-DD:BDNF is being packaged into AAV2 to localize spatial transduction spread and AAV9 serotype to optimize infectivity of brain and spinal cord tissue.

Dorsal Root Ganglia Extraction, Electroporation, and Culture

Adult Fischer 344 rats were anesthetized and decapitated. DRGs were then extracted, electroporated and cultured using the protocol described in McCall, 2012 #48. The DRGs were plated at 2 x 10^5 cells/mL and grown 7 DIV (days *in vitro*) before drug timecourse experiments. TMP (Trimethoprim) was added at a final media volume of 10uM to each well containing electroporated cells. Timecourse conditions were as follows: 24 hours TMP, 2 hours TMP, 0 hours TMP baseline control, 24 hours 10uM DMSO control, and p524 (AAV-CAG-BDNF) electroporated culture as a BDNF positive control. Following appropriate experimental conditions, supernatants from each well were collected and cells lysates were harvested were washed. DRGs were lysed using cell SDS lysis buffer: dPBS with 1% SDS, 1.5mM EGTA, 1.0mM EDTA, and a general protease inhibitor (Roche #14696200). Lysate were purified by sonication on ice and centrifugation to separate proteins from cell debris. The supernatant, containing desired proteins, was analyzed for protein concentration by A280 analysis on a NanoDrop 1000. Lysate proteins were then probed by Western blot, and by ELISA for secreted BDNF in the cell media.

293TAB transfection and TMP timecourse

293TAB cells were plated at a density of 600,000 cells/ mL at 37C, and the next day were PEI transfected with either p943 or p944. Cells were harvested on day 5 following 0, 1, 4, and 24 hours of 10uM TMP administration. Cell media supernatants were collected for later ELISA analysis, and cells were lysed with 1%SDS lysis buffer containing the same concentration of protease inhibitors mentioned in Chapter 2.2. Cell lysates were broken up by sonication, and protein purified by max centrifugation in preparation for Western blot.

Western Blot

Cell lysate BDNF was determined by Western blot following the ThermoFisher NuPage Western blot technical manual (NuPage IM-1001, pg. 35-53) and using Precision Plus Protein All Blue Prestained Protein Standards (Bio-Rad #1610373). Western blot antibody dilutions can be found in Table 2.

Chapter 4.3: DD-BDNF *in vitro* Results

To validate the destabilizing "DD" (degradation domain) fused onto the N- and C-terminal of BDNF, BDNF-DD (p943) and DD-BDNF (p944) transfected 293TAB cells underwent a TMP time course with collection of cell media supernatants and cell lysates. Untransfected cells are controls for transfection and the 1% DMSO found in TMP. ELISA was used to measure accumulated BDNF stably secreted in the presence of TMP, as shown in Figure 4.1.

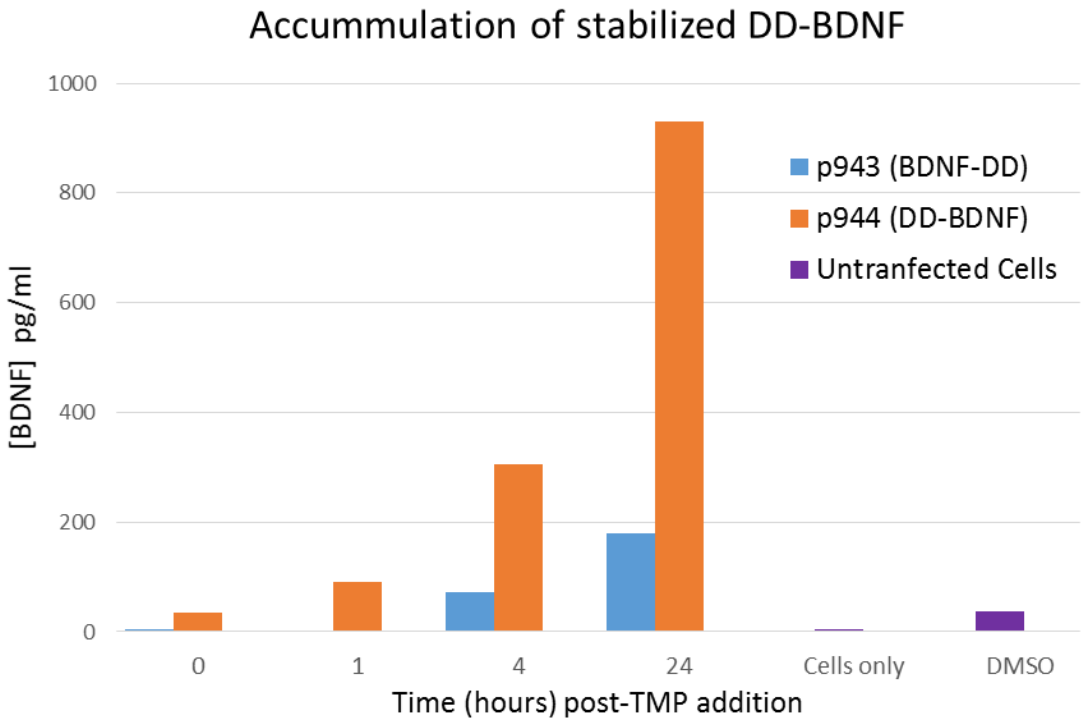

Figure 4.1: BDNF ELISA of DD-BDNF and BDNF-DD transfected 293TAB cell supernatants following TMP time course

Western blot of the 293TAB cell lysates (Figure 4.2) showed very low levels of BDNF in the absence of TMP, with leakiness most likely due to high plasmid copy numbers per cell from the electroporation driving DD-BDNF overexpression. Following drug addition,

High levels of DD-BDNF (N-terminal fusion) are rapidly and robustly induced by TMP until at least 4 hours, before returning to basal levels 24-hours post TMP treatment.

Interestingly, BDNF-DD, with the DHFR degradation domain fused to the C-terminal of BDNF, appears to show the opposite response to TMP addition. In the absence of TMP, BDNF-DD is expressed at high levels, demonstrating that it is not being degraded as expected. When TMP is added, very surprisingly, we observed a rapid and persistent reduction in BDNF-DD expression that continues over time up to 24 hours post TMP, indicating that the BDNF-DD protein is actually being de-stabilized and degraded in the PRESENCE of TMP rather than in the absence of TMP as described for the DD-BDNF construct, and as reported for other N-terminal DD-fusion proteins such as Cre, and EGFP (Sando et al, 2013 #49). So, by changing the location of the DD-tag on the BDNF protein we appear to have generated two constructs with opposite responses to TMP, namely a “TMP-OFF” BDNF-DD construct and a “TMP-ON” DD-BDNF construct. The exact mechanism behind these opposite responses is unclear, but highlights the importance of protein conformation on the ability of this approach to regulate protein levels in response to the activating drug. This surprising result suggests that when using this “DD” approach, each novel protein construct should be tested with the degradation domain on each end of the polypeptide to make sure that the kinetics of stabilization in the presence of TMP are as expected.

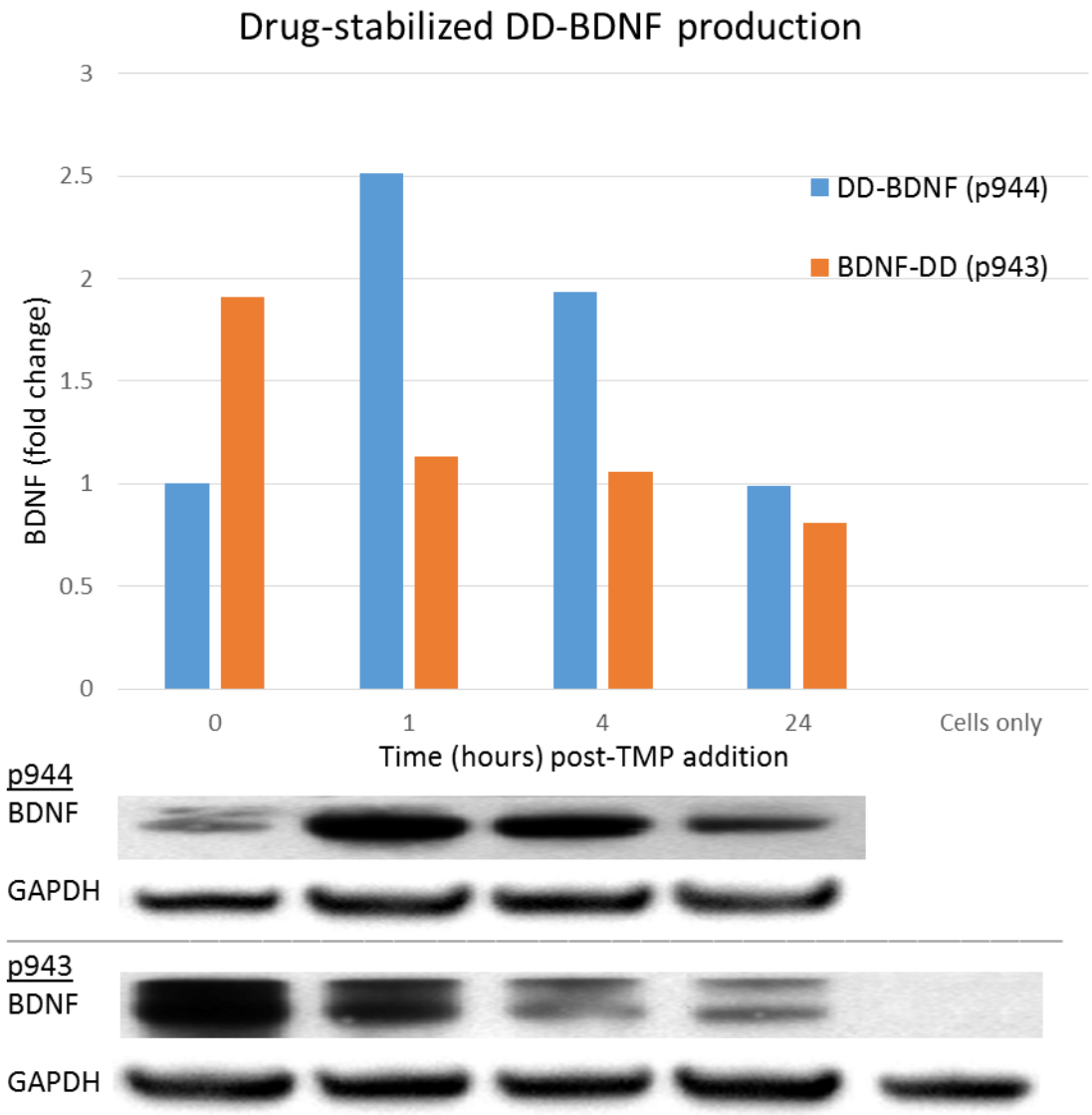

Figure 4.2: Western blot of 293TAB cells lysates transfected with p943 and p944 plasmids expressing BDNF-DD or DD-BDNF.

Chapter 4.4: DD-BDNF Discussion and Future Directions

I hypothesize that the DD-BDNF system *in vitro* would allow drug-regulated exogenous BDNF expression. This is similar to the elevated endogenous BDNF expression offered by the GsDREADD system, but is a more direct approach that expresses exogenous BDNF without the intermediary intracellular signaling pathways involved in cAMP regulation. In the DD-BDNF system, Figures 4.1 and 4.2 both show elevated BDNF following TMP addition for plasmids p944 (AAV-CAG-DD:BDNF) with the C-terminal fusion of the DHFR destabilizing domain. Plasmid p943 with the N-terminal fusion does not appear to be drug-elevated as expected, instead should stable expression in the absence of TMP, and rapid de-stabilization and degradation when TMP was added. Nonetheless, the presence of TMP in DD-BDNF production demonstrated protein stabilization and expression at robust exogenous levels. Potentially DD-BDNF could promote stable BDNF expression and secretion *in vivo* when TMP is given systemically, and also allow withdrawal of BDNF therapy at the conclusion of spinal cord injury treatment. I will continue with the p944 DD-BDNF system as a regulator of exogenous BDNF that could be therapeutically relevant to models of SCI.

While the DD-BDNF method does not activate cAMP intracellular signaling that promotes neuroprotection and growth, it is “cleaner” by not activating many intracellular signaling pathways that could potentially have off-target outcomes. Similar to GsDREADD *in vitro* methods, DD-BDNF was cloned into an rCOMET-expressing AAV plasmid and is currently being virally packaged into AAV2 and AAV8 for localized and distributed spread in the central nervous system, respectively. I am currently replicating the DD-BDNF plasmid in a model of adult central nervous system that normally secretes BDNF: DRG (Dorsal Root Ganglion) culture electroporation. I plan to investigate DD-

BDNF DRG culture using similar time points for drug-exposure. The 24 hour time course should be sufficient for an in vivo model of inducible BDNF expression because TMP is a common antibiotic that would have little off-target effects. Finally, I plan to address Aim 2 (*in vivo* validation in an uninjured model) next with DD-BDNF when DD-BDNF AAV creation is complete, but was unable to complete this within my Master's study.

Tables

Table 1: AAV Plasmids and Viral Titers

Plasmid	Description	Viral Titer (GC/mL)	Gene of Interest	Reporter
p524	AAV-CAG-BDNF	AAV2 3.7 x 10^{12}	BDNF	None
p943	AAV-CAG-BDNF:DD	N/A	BDNF:DD	None
p944	AAV-CAG-DD:BDNF	N/A	DD:BDNF	None
p976	AAV-CAG-gCOMET-GsDREADD	AAV8 1.27 x 10^{12}	GsDREADD	gCOMET
p976	AAV-CAG-gCOMET-GsDREADD	AAV2 1.25 x 10^{11}	GsDREADD	gCOMET
p1112	AAV-CAG-rCOMET-GsDREADD	AAV2 6.47 x 10^{11}	GsDREADD	rCOMET

Table 2: Western Blot Antibodies

Antibody	Species	Dilution	Source
B-actin	Mouse	1:5000	Sigma-Aldrich
B3-Tubulin	Mouse	1:5000	Cell Signaling
BDNF	Rabbit	1:1000	Chicago-Ling
CREB	Rabbit	1:1000	Cell Signaling
ERK	Rabbit	1:1000	Cell Signaling
P-CREB	Rabbit	1:1000	Cell Signaling
P-ERK	Rabbit	1:1000	Cell Signaling

Table 3: Immunohistochemistry Antibodies

Antibody	Species	Dilution	Specificity	Source
β3-Tubulin	Mouse	1:1000	Beta-III Tubulin, neuronal cytoskeleton	Abcam
BDNF	Rabbit	1:5000 LL, 1:1000 Fluor	Brain-Derived Neurotrophic Factor	Chicago-Ling
CTB	Mouse	1:200 Fluor	Cholera Toxin b subunit	SigmaAldrich
GFP	Rabbit	1:400 Fluor	Green Fluorescent Protein	Cell Signaling
Brn3A	Rabbit	1:500 Fluor	Most retinal cells; Transcription factor	Santa Cruz Biotech
DAPI	N/A	1:1000 Fluor	All nuclei	Unknown
NeuN	Goat	1:500 Fluor	Most mature neuronal nuclei	Millipore

Table 4: Plasmid Maps

p943: AAV-CAG-gCOMET-BDNF:DD

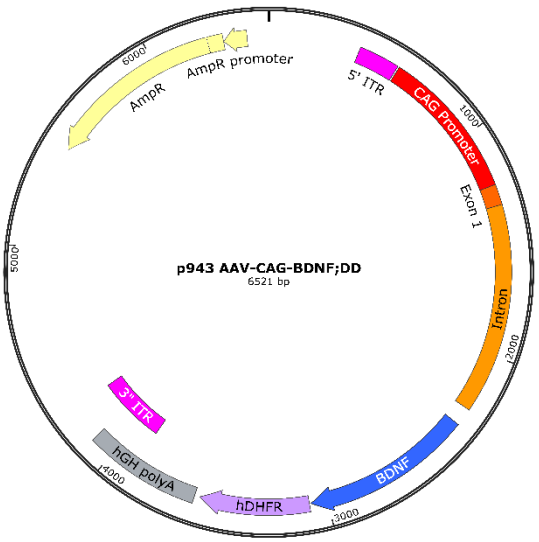

p944: AAV-CAG-gCOMET-DD:BDNF

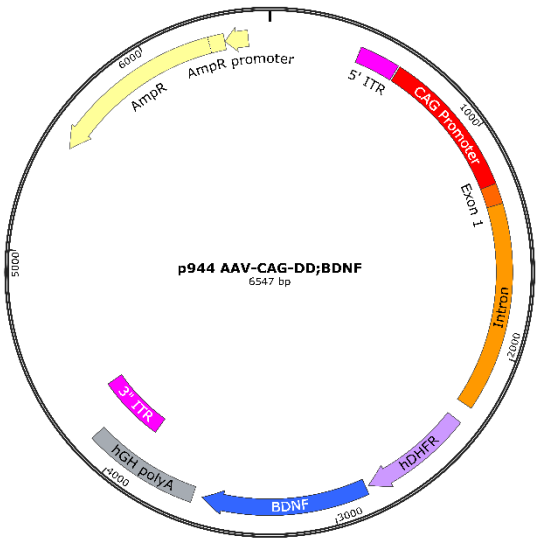

p976: AAV-CAG-gCOMET-GsDREADD

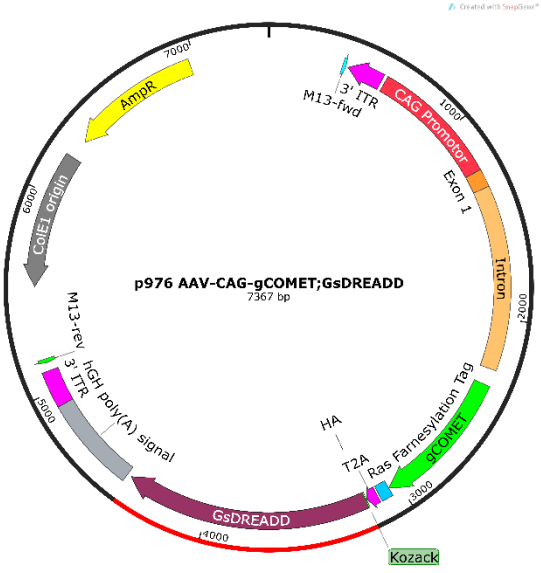

p1112: AAV-CAG-rCOMET-GsDREADD

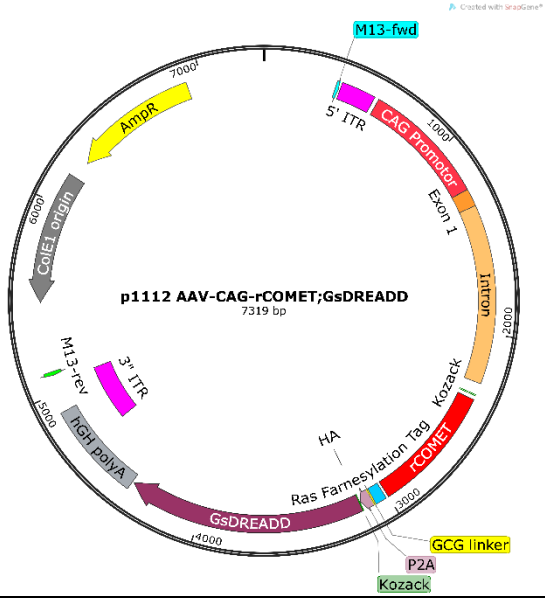

References

1 F. Akbik, W. B. Cafferty, and S. M. Strittmatter, 'Myelin Associated Inhibitors: A Link between Injury-Induced and Experience-Dependent Plasticity', *Exp Neurol,* 235 (2012), 43-52.

2 BioResearch, 'Amaxa™ 4d-Nucleofector™ Protocol for Rat Hippocampal or Cortical Neurons', ed. by Lonza (Lonza Cologne GmbH: 2012), pp. 1-5.

3 A. Blesch, P. Lu, S. Tsukada, L. T. Alto, K. Roet, G. Coppola, D. Geschwind, and M. H. Tuszynski, 'Conditioning Lesions before or after Spinal Cord Injury Recruit Broad Genetic Mechanisms That Sustain Axonal Regeneration: Superiority to Camp-Mediated Effects', *Exp Neurol,* 235 (2012), 162-73.

4 A. Blesch, P. Lu, and M. H. Tuszynski, 'Neurotrophic Factors, Gene Therapy, and Neural Stem Cells for Spinal Cord Repair', *Brain Res Bull,* 57 (2002), 833-8.

5 J. F. Bonner, T. M. Connors, W. F. Silverman, D. P. Kowalski, M. A. Lemay, and I. Fischer, 'Grafted Neural Progenitors Integrate and Restore Synaptic Connectivity across the Injured Spinal Cord', *J Neurosci,* 31 (2011), 4675-86.

6 J. H. Brock, E. S. Rosenzweig, A. Blesch, R. Moseanko, L. A. Havton, V. R. Edgerton, and M. H. Tuszynski, 'Local and Remote Growth Factor Effects after Primate Spinal Cord Injury', *J Neurosci,* 30 (2010), 9728-37.

7 M. J. Castle, Z. T. Gershenson, A. R. Giles, E. L. Holzbaur, and J. H. Wolfe, 'Adeno-Associated Virus Serotypes 1, 8, and 9 Share Conserved Mechanisms for Anterograde and Retrograde Axonal Transport', *Hum Gene Ther,* 25 (2014), 705-20.

8 National Spinal Cord Injury Statistical Center, 'Facts and Figures at a Glance', (Birmingham, AL: University of Alabama at Birmingham, 2015).

9 M. J. Chen, T. V. Nguyen, C. J. Pike, and A. A. Russo-Neustadt, 'Norepinephrine Induces Bdnf and Activates the Pi-3k and Mapk Cascades in Embryonic Hippocampal Neurons', *Cell Signal,* 19 (2007), 114-28.

10 P. L. Cheng, A. H. Song, Y. H. Wong, S. Wang, X. Zhang, and M. M. Poo, 'Self-Amplifying Autocrine Actions of Bdnf in Axon Development', *Proc Natl Acad Sci U S A,* 108 (2011), 18430-5.

11 T. Cheriyan, D. J. Ryan, J. H. Weinreb, J. Cheriyan, J. C. Paul, V. Lafage, T. Kirsch, and T. J. Errico, 'Spinal Cord Injury Models: A Review', *Spinal Cord,* 52 (2014), 588-95.

12 S. Cohen-Cory, A. H. Kidane, N. J. Shirkey, and S. Marshak, 'Brain-Derived Neurotrophic Factor and the Development of Structural Neuronal Connectivity', *Dev Neurobiol,* 70 (2010), 271-88.

13 J. D. Ding, X. Y. Tang, J. G. Shi, and L. S. Jia, 'Bdnf-Mediated Modulation of Glycine Transmission on Rat Spinal Motoneurons', *Neurosci Lett,* 578 (2014), 95-9.

14 M. L. Donnelly, L. E. Hughes, G. Luke, H. Mendoza, E. ten Dam, D. Gani, and M. D. Ryan, 'The 'Cleavage' Activities of Foot-and-Mouth Disease Virus 2a Site-Directed Mutants and Naturally Occurring '2a-Like' Sequences', *J Gen Virol,* 82 (2001), 1027-41.

15 M. S. Farrell, Y. Pei, Y. Wan, P. N. Yadav, T. L. Daigle, D. J. Urban, H. M. Lee, N. Sciaky, A. Simmons, R. J. Nonneman, X. P. Huang, S. J. Hufeisen, J. M. Guettier, S. S. Moy, J. Wess, M. G. Caron, N. Calakos, and B. L. Roth, 'A Galphas Dreadd Mouse for Selective Modulation of Camp Production in Striatopallidal Neurons', *Neuropsychopharmacology,* 38 (2013), 854-62.

16 K. Fouad, D. J. Bennett, R. Vavrek, and A. Blesch, 'Long-Term Viral Brain-Derived Neurotrophic Factor Delivery Promotes Spasticity in Rats with a Cervical Spinal Cord Hemisection', *Front Neurol,* 4 (2013), 187.

17 M. Gao, P. Lu, B. Bednark, D. Lynam, J. M. Conner, J. Sakamoto, and M. H. Tuszynski, 'Templated Agarose Scaffolds for the Support of Motor Axon Regeneration into Sites of Complete Spinal Cord Transection', *Biomaterials,* 34 (2013), 1529-36.

18 C. G. Geoffroy, and B. Zheng, 'Myelin-Associated Inhibitors in Axonal Growth after Cns Injury', *Curr Opin Neurobiol,* 27 (2014), 31-8.

19 A. Ghosh-Roy, Z. Wu, A. Goncharov, Y. Jin, and A. D. Chisholm, 'Calcium and Cyclic Amp Promote Axonal Regeneration in Caenorhabditis Elegans and Require Dlk-1 Kinase', *J Neurosci,* 30 (2010), 3175-83.

20 L. C. Gill, H. M. Gransee, G. C. Sieck, and C. B. Mantilla, 'Functional Recovery after Cervical Spinal Cord Injury: Role of Neurotrophin and Glutamatergic Signaling in Phrenic Motoneurons', *Respir Physiol Neurobiol* (2015).

21 S. S. Hannila, and M. T. Filbin, 'The Role of Cyclic Amp Signaling in Promoting Axonal Regeneration after Spinal Cord Injury', *Exp Neurol,* 209 (2008), 321-32.

22 M. Hellstrom, and A. R. Harvey, 'Cyclic Amp and the Regeneration of Retinal Ganglion Cell Axons', *Int J Biochem Cell Biol,* 56 (2014), 66-73.

23 L. L. Jones, Y. Yamaguchi, W. B. Stallcup, and M. H. Tuszynski, 'Ng2 Is a Major Chondroitin Sulfate Proteoglycan Produced after Spinal Cord Injury and Is Expressed by Macrophages and Oligodendrocyte Progenitors', *J Neurosci,* 22 (2002), 2792-803.

24 K. Kadoya, S. Tsukada, P. Lu, G. Coppola, D. Geschwind, M. T. Filbin, A. Blesch, and M. H. Tuszynski, 'Combined Intrinsic and Extrinsic Neuronal Mechanisms Facilitate Bridging Axonal Regeneration One Year after Spinal Cord Injury', *Neuron,* 64 (2009), 165-72.

25 A. Kaplan, S. Ong Tone, and A. E. Fournier, 'Extrinsic and Intrinsic Regulation of Axon Regeneration at a Crossroads', *Front Mol Neurosci,* 8 (2015), 27.

26 C. H. Lou, A. Shao, E. Y. Shum, J. L. Espinoza, L. Huang, R. Karam, and M. F. Wilkinson, 'Posttranscriptional Control of the Stem Cell and Neurogenic Programs by the Nonsense-Mediated Rna Decay Pathway', *Cell Rep,* 6 (2014), 748-64.

27 P. Lu, A. Blesch, L. Graham, Y. Wang, R. Samara, K. Banos, V. Haringer, L. Havton, N. Weishaupt, D. Bennett, K. Fouad, and M. H. Tuszynski, 'Motor Axonal Regeneration after Partial and Complete Spinal Cord Transection', *J Neurosci,* 32 (2012), 8208-18.

28 P. Lu, L. L. Jones, E. Y. Snyder, and M. H. Tuszynski, 'Neural Stem Cells

Constitutively Secrete Neurotrophic Factors and Promote Extensive Host Axonal Growth after Spinal Cord Injury', *Exp Neurol,* 181 (2003), 115-29.

29 P. Lu, L. L. Jones, and M. H. Tuszynski, 'Axon Regeneration through Scars and into Sites of Chronic Spinal Cord Injury', *Exp Neurol,* 203 (2007), 8-21.

30 P. Lu, K. Kadoya, and M. H. Tuszynski, 'Bdnf-Expressing Marrow Stromal Cells Support Extensive Axonal Growth at Sites of Spinal Cord Injury', *Exp Neurol,* 191 (2005), 344-60.

31 P. Lu, K. Kadoya, and M. H. Tuszynski, 'Axonal Growth and Connectivity from Neural Stem Cell Grafts in Models of Spinal Cord Injury', *Curr Opin Neurobiol,* 27 (2014), 103-9.

32 P. Lu, and M. H. Tuszynski, 'Can Bone Marrow-Derived Stem Cells Differentiate into Functional Neurons?', *Exp Neurol,* 193 (2005), 273-8.

33 P. Lu, and M. H. Tuszynski, 'Growth Factors and Combinatorial Therapies for Cns Regeneration', *Exp Neurol,* 209 (2008), 313-20.

34 P. Lu, Y. Wang, L. Graham, K. McHale, M. Gao, D. Wu, J. Brock, A. Blesch, E. S. Rosenzweig, L. A. Havton, B. Zheng, J. M. Conner, M. Marsala, and M. H. Tuszynski, 'Long-Distance Growth and Connectivity of Neural Stem Cells after Severe Spinal Cord Injury', *Cell,* 150 (2012), 1264-73.

35 P. Lu, H. Yang, L. L. Jones, M. T. Filbin, and M. H. Tuszynski, 'Combinatorial Therapy with Neurotrophins and Camp Promotes Axonal Regeneration Beyond Sites of Spinal Cord Injury', *J Neurosci,* 24 (2004), 6402-9.

36 J. Mai, L. Fok, H. Gao, X. Zhang, and M. M. Poo, 'Axon Initiation and Growth Cone Turning on Bound Protein Gradients', *J Neurosci,* 29 (2009), 7450-8.

37 J. McCall, L. Nicholson, N. Weidner, and A. Blesch, 'Optimization of Adult Sensory Neuron Electroporation to Study Mechanisms of Neurite Growth', *Front Mol Neurosci,* 5 (2012), 11.

38 O. K. Melemedjian, D. V. Tillu, J. K. Moy, M. N. Asiedu, E. K. Mandell, S. Ghosh,

G. Dussor, and T. J. Price, 'Local Translation and Retrograde Axonal Transport of Creb Regulates Il-6-Induced Nociceptive Plasticity', *Mol Pain,* 10 (2014), 45.

39 G. L. Ming, S. T. Wong, J. Henley, X. B. Yuan, H. J. Song, N. C. Spitzer, and M. M. Poo, 'Adaptation in the Chemotactic Guidance of Nerve Growth Cones', *Nature,* 417 (2002), 411-8.

40 A. H. Nagahara, D. A. Merrill, G. Coppola, S. Tsukada, B. E. Schroeder, G. M. Shaked, L. Wang, A. Blesch, A. Kim, J. M. Conner, E. Rockenstein, M. V. Chao, E. H. Koo, D. Geschwind, E. Masliah, A. A. Chiba, and M. H. Tuszynski, 'Neuroprotective Effects of Brain-Derived Neurotrophic Factor in Rodent and Primate Models of Alzheimer's Disease', *Nat Med,* 15 (2009), 331-7.

41 S. A. Nicklin, H. Buening, K. L. Dishart, M. de Alwis, A. Girod, U. Hacker, A. J. Thrasher, R. R. Ali, M. Hallek, and A. H. Baker, 'Efficient and Selective Aav2-Mediated Gene Transfer Directed to Human Vascular Endothelial Cells', *Mol Ther,* 4 (2001), 174-81.

42 H. Park, and M. M. Poo, 'Neurotrophin Regulation of Neural Circuit Development and Function', *Nat Rev Neurosci,* 14 (2013), 7-23.

43 K. K. Park, K. Liu, Y. Hu, P. D. Smith, C. Wang, B. Cai, B. Xu, L. Connolly, I. Kramvis, M. Sahin, and Z. He, 'Promoting Axon Regeneration in the Adult Cns by Modulation of the Pten/Mtor Pathway', *Science,* 322 (2008), 963-6.

44 L. M. Pettersson, N. M. Geremia, Z. Ying, and V. M. Verge, 'Injury-Associated Pacap Expression in Rat Sensory and Motor Neurons Is Induced by Endogenous Bdnf', *PLoS One,* 9 (2014), e100730.

45 C. Phillips, M. A. Baktir, M. Srivatsan, and A. Salehi, 'Neuroprotective Effects of Physical Activity on the Brain: A Closer Look at Trophic Factor Signaling', *Front Cell Neurosci,* 8 (2014), 170.

46 D. E. Read, and A. M. Gorman, 'Involvement of Akt in Neurite Outgrowth', *Cell Mol Life Sci,* 66 (2009), 2975-84.

47 L. F. Reichardt, 'Neurotrophin-Regulated Signalling Pathways', *Philos Trans R Soc Lond B Biol Sci,* 361 (2006), 1545-64.

48 M. B. Rosenberg, T. Friedmann, R. C. Robertson, M. Tuszynski, J. A. Wolff, X. O. Breakefield, and F. H. Gage, 'Grafting Genetically Modified Cells to the Damaged Brain: Restorative Effects of Ngf Expression', *Science,* 242 (1988), 1575-8.

49 R. Sando, 3rd, K. Baumgaertel, S. Pieraut, N. Torabi-Rander, T. J. Wandless, M. Mayford, and A. Maximov, 'Inducible Control of Gene Expression with Destabilized Cre', *Nat Methods,* 10 (2013), 1085-8.

50 M. M. Siddiq, and S. S. Hannila, 'Looking Downstream: The Role of Cyclic Amp-Regulated Genes in Axonal Regeneration', *Front Mol Neurosci,* 8 (2015), 26.

51 M. V. Sofroniew, 'Reactive Astrocytes in Neural Repair and Protection', *Neuroscientist,* 11 (2005), 400-7.

52 H. J. Song, G. L. Ming, and M. M. Poo, 'Camp-Induced Switching in Turning Direction of Nerve Growth Cones', *Nature,* 388 (1997), 275-9.

53 F. Sun, K. K. Park, S. Belin, D. Wang, T. Lu, G. Chen, K. Zhang, C. Yeung, G. Feng, B. A. Yankner, and Z. He, 'Sustained Axon Regeneration Induced by Co-Deletion of Pten and Socs3', *Nature,* 480 (2011), 372-5.

54 X. Tao, S. Finkbeiner, D. B. Arnold, A. J. Shaywitz, and M. E. Greenberg, 'Ca2+ Influx Regulates Bdnf Transcription by a Creb Family Transcription Factor-Dependent Mechanism', *Neuron,* 20 (1998), 709-26.

55 W. Tetzlaff, E. B. Okon, S. Karimi-Abdolrezaee, C. E. Hill, J. S. Sparling, J. R. Plemel, W. T. Plunet, E. C. Tsai, D. Baptiste, L. J. Smithson, M. D. Kawaja, M. G. Fehlings, and B. K. Kwon, 'A Systematic Review of Cellular Transplantation Therapies for Spinal Cord Injury', *J Neurotrauma,* 28 (2011), 1611-82.

56 M. H. Tuszynski, R. Grill, L. L. Jones, A. Brant, A. Blesch, K. Low, S. Lacroix, and P. Lu, 'Nt-3 Gene Delivery Elicits Growth of Chronically Injured Corticospinal Axons and Modestly Improves Functional Deficits after Chronic Scar Resection', *Exp Neurol,* 181 (2003), 47-56.

57 M. H. Tuszynski, L. Thal, M. Pay, D. P. Salmon, H. S. U, R. Bakay, P. Patel, A. Blesch, H. L. Vahlsing, G. Ho, G. Tong, S. G. Potkin, J. Fallon, L. Hansen, E. J.

Mufson, J. H. Kordower, C. Gall, and J. Conner, 'A Phase 1 Clinical Trial of Nerve Growth Factor Gene Therapy for Alzheimer Disease', *Nat Med,* 11 (2005), 551-5.

58 G. Umschweif, S. Liraz-Zaltsman, D. Shabashov, A. Alexandrovich, V. Trembovler, M. Horowitz, and E. Shohami, 'Angiotensin Receptor Type 2 Activation Induces Neuroprotection and Neurogenesis after Traumatic Brain Injury', *Neurotherapeutics,* 11 (2014), 665-78.

59 N. Weidner, A. Ner, N. Salimi, and M. H. Tuszynski, 'Spontaneous Corticospinal Axonal Plasticity and Functional Recovery after Adult Central Nervous System Injury', *Proc Natl Acad Sci U S A,* 98 (2001), 3513-8.

60 W. K. Wong, A. W. Cheung, S. W. Yu, O. Sha, and E. Y. Cho, 'Hepatocyte Growth Factor Promotes Long-Term Survival and Axonal Regeneration of Retinal Ganglion Cells after Optic Nerve Injury: Comparison with Cntf and Bdnf', *CNS Neurosci Ther,* 20 (2014), 916-29.

61 X. M. Xu, V. Guenard, N. Kleitman, P. Aebischer, and M. B. Bunge, 'A Combination of Bdnf and Nt-3 Promotes Supraspinal Axonal Regeneration into Schwann Cell Grafts in Adult Rat Thoracic Spinal Cord', *Exp Neurol,* 134 (1995), 261-72.

62 H. Yang, P. Lu, H. M. McKay, T. Bernot, H. Keirstead, O. Steward, F. H. Gage, V. R. Edgerton, and M. H. Tuszynski, 'Endogenous Neurogenesis Replaces Oligodendrocytes and Astrocytes after Primate Spinal Cord Injury', *J Neurosci,* 26 (2006), 2157-66.